Aus der Medizinischen Klinik für Hepatologie und Gastroenterologie,
Campus Virchow Klinikum
der Medizinischen Fakultät Charité-Universitätsmedizin Berlin

In Kollaboration mit:
Michael Geoffrey Rosenfeld, University of California, San Diego

DISSERTATION

Identification and characterization of potential target genes of the histone demethylase PTDSR/JMJD6

zur Erlangung des akademischen Grades
Doctor medicinae (Dr. med.)

vorgelegt der Medizinischen Fakultät
Charité – Universitätsmedizin Berlin

von
Ania Lisette Berdel
aus Berlin

Gutachter: 1. Priv.-Doz. Dr. med. T. Cramer

2. Prof. Dr. rer. nat. A. Leutz

3. Prof. M. G. Rosenfeld

Datum der Promotion: 30. November 2012

Table of contents

Content

List of figures

List of tables

List of abbreviations

AP	anterior-posterior polarity
AR	Androgen receptor
Bp	Base pare
cDNA	complementary DNA
ChIP	Chromatin immunoprecipitation
CNS	Central nervous system
CO2	Carbon dioxide
DMEM	Dulbecco's modified Eagle's medium
DNMT	DNA methyltransferase
ECL	Enhanced luminal-based chemiluminescent
FDR	False Discovery Rate
h	Hour
H2O	Water
HkG	Housekeeping gene
HMT	Histone Methyltransferases
JARID	JmjC domain containing proteins
JHDM1	JmjC domain containing histone demethylases
JmjC	Jumonji C domain containing enzymes
LSD1	Lysine specific demethylase 1
MCS	multiple coning sites
me1	monomethylated
me2	dimethylated
me3	trimethylated
mg	milligrams
min	minute
mRNA	messenger RNA
ncRNA	non-coding RNA
ng	nanograms
PRMT	Protein arginine methyltransferases
PTDSR	Phosphatidylserine receptor/ JMJD6
RIP	RNA-immunoprecipitation
RNA	Ribonucleic Acid
RNAi	RNA interference
RNA-seq	RNA-sequencing
Rpm	Rotations per minute
RT-qPCR	Reverse Transcriptase/quantitative PCR

shRNA	short hairpin RNA
siRNA	small interfering RNA
TF	Transcription factor
UTR	Untranslated region
UV	Ultra violet light
V	Volt

1. Introduction

1.1. Epigenetics and organization of the chromatin

The center focus of genetics is the DNA, its organization within genes and regulatory sequences, its alteration through mutation and inheritance to the next generation. In biology, the term epigenetics refers to changes in gene expression that are controlled by heritable but potentially reversible changes in DNA modification and/or chromatin structure. Chromatin is the complex of nucleic acid (DNA) and proteins (histones) in eukaryotic cells that is usually dispersed in the interphase nucleus and condensed into chromosomes in mitosis and meiosis. There are two major epigenetic mechanisms, which also may be linked together, playing an important role in the influence of gene expression. On the one hand there is the chromatin structure as a means to control gene expression and on the other hand there is the DNA methylation in these structural changes, especially in its promoter region, that influences gene expression (also see 1.1.2.).
The events that affect chromatin structure can be defined as epigenetic events.

A major way of cell differentiation is through a process of activating (turning “on”) some genes while silencing (turning “off”) others. Epigenetic mechanisms enforcing accessibility of genetic material, such as changes in chromatin structure and DNA methylation are the foundation of cell differentiation. (She X et al, 2009).
These alterations of the DNA are not changes in the actual DNA sequence of the organism, instead, environmental factors may cause the organism’s genes to be regulated and expressed differently (Shi Y et al, 2007). It is currently well accepted that epigenetics play a central role in regulation, differentiation and development of mammalian cells.

In order to store the genome in the nucleus of eukaryotic cells, it is important to package the DNA into chromatin. Chromatin is able to undergo dynamic changes during replication, recombination, transcription and DNA repair, but also to control temporal gene expression. Histone proteins are found in the cell nucleus of eukaryotes and acquire packaging of the DNA, providing a cornerstone of regulation for gene expression (Van Holde KE, 1988). The histone itself is the evolutionarily conserved

building block of chromatin, and consists of the nucleosomal core particle containing a histone octamer (comprised of H2A, H2B, H3, and H4) around which 147bp of DNA are wrapped (Fig.01). Linker histone H1 binds to the DNA between the nucleosomal core particles and stabilizes higher order chromatin structure (Daujat S et al, 2005).

Posttranslational modifications are capable of regulating chromatin architecture and can affect all aspects of DNA processing, resulting in explicit outcomes concerning chromatin–dependent functions such as gene expression (Jenuwein T et al, 2001; Strahl BD et al, 2000). The epigenetic mechanisms working together in order to control gene regulation and cellular morphology include: histone modifications, DNA methylation, chromatin condensation and small RNAs (Radman-Livaja, 2009).

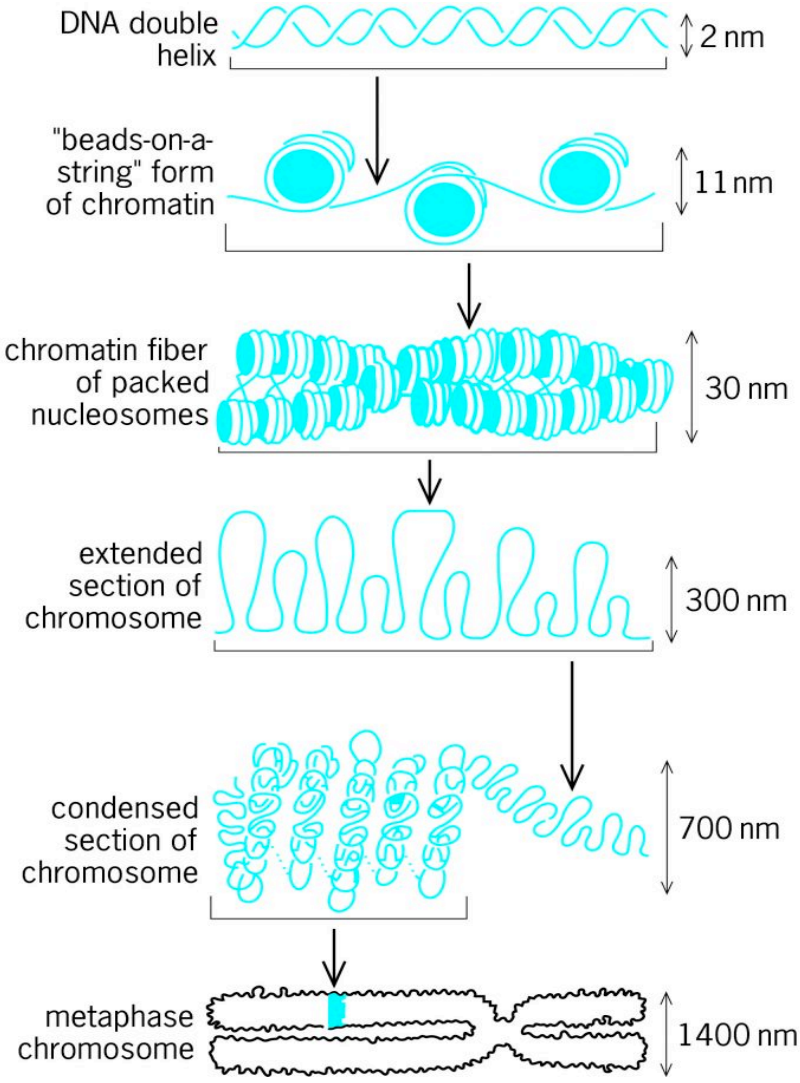

Fig.01: Organization of DNA into chromosomes: The complex of DNA and histones build the nucleosome. Further condensation leads to euchromatin (active) and heterochromatin (inactive), up to the final unit, the chromosome (Alberts B et al., Molecular Biology of the Cell, 2d ed., Garland Publishing, 1989)

1.1.1. Histone modification

Covalent modifications on histones play an important role in the regulation of chromatin dynamics and function and are linked to transcriptional activation as well as repression. Several types of post-translational modifications have been identified on histones, the four most common ones being acetylation, methylation, phosphorylation and ubiquitination as illustrated in Fig.02 (Hahn P et al, 2010; Emre NC et al, 2006). DNA methylation is likely to be the most important epigenetic event controlling and importantly maintaining the pattern of gene expression during development. Histone methylation, being of particular interest, occurs on both lysine and arginine residues, and has been linked to DNA methylation and strongly implicated in epigenetic regulation, affecting the transcription of specific genes.

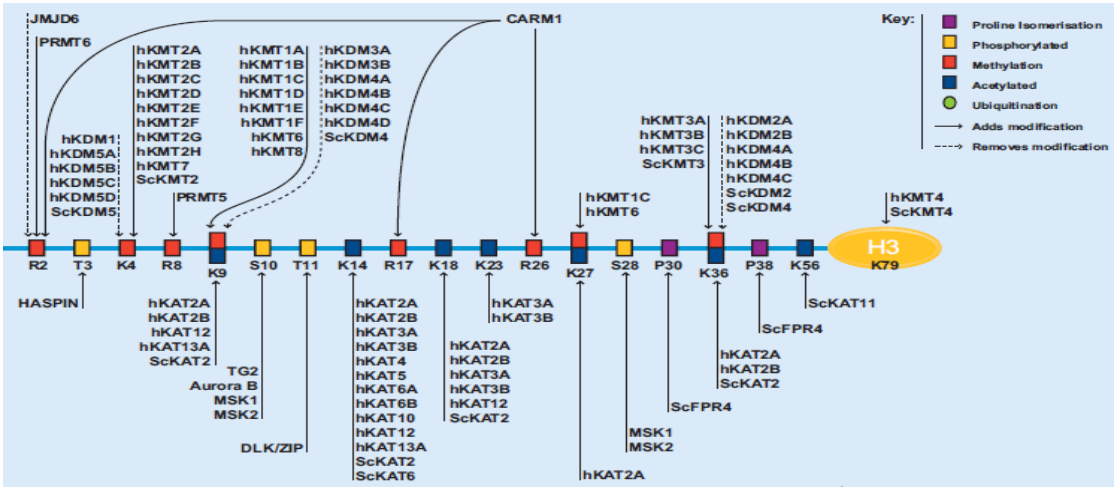

Fig.02: Modifications on Histone H3 (Homo sapiens): Schematic representation of known modifications on histone H3 and their corresponding modifying enzymes (www.abcam.com).

Recently, several enzymes have been characterized to catalyze the methylation of histone lysine and arginine residues, which have been shown to be required for normal development of several organs and play a key role in the development of diseases such as cancer (Paul AC et al, 2011; Robertson KD, 2005). Many of the covalent modifications taking place on the histone tails are enzymatically reversible. For example phosphorylation and acetylation are reversed by phosphatases and deacetylases, respectively. This enzyme-based reversibility enables the cell to respond quickly to changes through rapid alterations in its gene expression programs.

Unlike histone acetylation and phosphorylation, histone methylation through histone methyltransferases (HMTase) was considered static and enzymatically irreversible. A study of a co-repressor (CoREST) led to the identification of the first histone demethylase LSD1 (Shi Y et al, 2004). Since then, the largest class of demethylase enzymes containing a Jumonji C (JmjC) domain was discovered (Tsukada Y et al, 2006). Identification and characterization of these enzymes provides new opportunities and challenges to understand histone methylation and the complex nature of chromatin regulation. Histone demethylases are likely to impact many biological processes, including stem cell maintenance and differentiation, genome integrity, X-chromosome inactivation and imprinting, cell-cycle regulation, tissue development, and differentiation, among others (Shi Y et al, 2007). In this thesis we have focused on identifying potential targets for the proposed demethylase JMJD6/PTDSR and on making out a possible regulation pattern.

1.1.2. Methylation of DNA template and lysine/arginine residues on histones

DNA methylation is a post-replication process, by which cytosine residues in CpG-rich sequences are methylated, forming gene-specific methylation patterns (Fig.03). Housekeeping genes (HkG), which are involved in basic functions needed for the sustenance of the cell, are constitutively expressed (they are always turned ON). They possess CpG-rich islands at the promoter region that are unmethylated in all cell types, reflecting a transcriptionally active state, whereas tissue-specific genes are methylated in all tissues except the tissue where the gene is expressed.

In general, a strong methylation state of a gene correlates with repression whereas low methylation is associated with activation, by which cells maintain their basic and tissue-specific functions, respectively (Xinwei S et al, 2009). These epigenetic changes are stable over rounds of cell division but do not involve changes in the underlying DNA sequence of the organism. It is important to note that epigenetic changes are not mutations. Sometimes the changes last for several generations. A good example of epigenetic change in eukaryotic biology is the process of cellular differentiation. During morphogenesis, totipotent stem cells become various pluripotent cell lines of the embryo, which then become fully differentiated cells. The cells differentiate by a process of activating some genes while silencing others, despite all cells containing the same

genetic material. Epigenetic mechanisms enforcing accessibility and usage of the genetic material are the foundation of cell differentiation (Xinwei S et al, 2009).

Histone methylation regulates fundamental processes such as heterochromatin formation, X chromosome inactivation, genomic imprinting, transcriptional regulation and DNA repair (Margueron R et al, 2005; Lachner M et al, 2002). By adding or removing methyl groups from the tails of histones, gene expression may be silenced or activated based on the lysine residues, which have been marked (Fig.02).

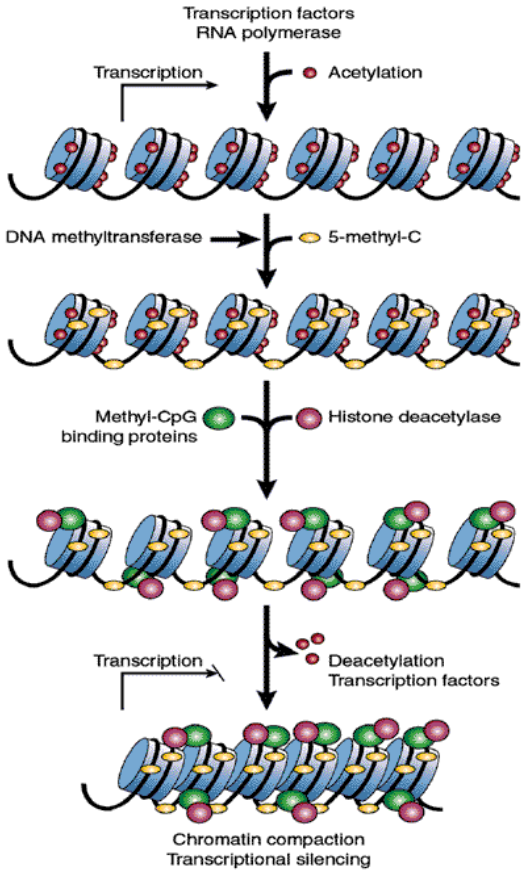

Fig.03: DNA methylation and acetylation.
(http://www.med.ufl.edu/biochem/keithr/research.html)

There is a specific code for the methylation status of histones which may be methylated on either lysine (K) (Murray K, 1964) or arginine (R) (Paik WK et al, 1967) residues. Lysine side chains may be mono- (me1), di- (me2) or tri-methylated (me3), whereas arginine side chains may be mono-methylated or symmetrically or asymmetrically di-methylated (Gary JD, 1998). Figs.04a and 04b show the chemical changes of lysine and arginine residues, respectively.

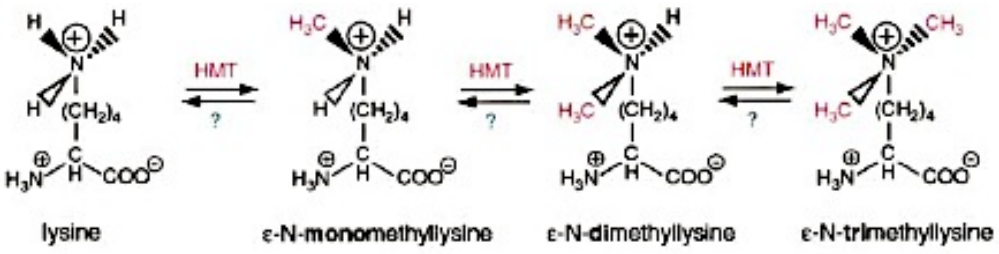

Fig.04a: Lysine methylation. Chemical structure of mono-, di-, and trimethylation of lysine residues through histone methyltransferases (HMTs). The potentinal reversibility of the reaction by demethylases is indicated with question marks (Bannister AJ et al, 2002).

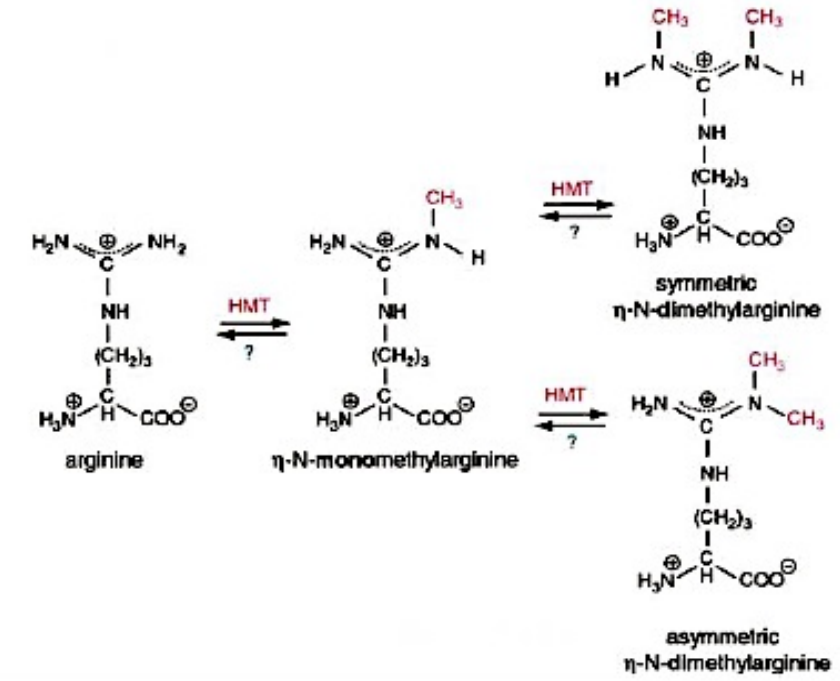

Fig.04b: Arginine methylation. Chemical structures of arginine and its methylated derivatives. The two forms in which dimethylarginine can be found are symmetric or asymmetric (Bannister AJ et al, 2002).

The protein arginine methylation is catalyzed by a family of enzymes called protein arginine methyltransferases (PRMTs). The PRMT family has been shown to include at least nine methyltransferases, designated as PRMT 1-9 based on differences in primary sequences and substrate specificity (Fig.02) (Pahlich S et al, 2006). Histone arginine methylation in general correlates with transcriptional activation of genes, whereas histone lysine methylation leads to either activation or repression, depending upon the particular lysine residue (Kouzarides T et al, 2002; Fischle W et al, 2003).

Histone lysine (K) methylation at H3K4, H3K36, and H3K79 has been linked to transcriptional activation (Martin C, 2005; Schubeler D, 2004; Krogan NJ, 2003; Nielsen SJ, 2001). In contrast, methylation at H3K9, H3K27, and H4K20, is associated with

repression of euchromatic genes (Schotta G, 2004; Reinberg D, 2004; Peters AH, 2003; Rice JC, 2003; Cao R, 2002; Nielsen SJ, 2001). Even within the same lysine residue, the biological consequence of methylation is variable, depending on the methylation state (Fig.02) (Santos-Rosa H et al, 2002; Wang H et al, 2003, Lachner M et al, 2004).

In conjunction with the expanding number of proteins that are known to be arginine methylated, a growing list of biological processes have been shown to involve arginine methylation, which include transcription, RNA processing and transport, translation, signal transduction, DNA repair and apoptosis (Lee DY et al, 2005; Gedford MT et al, 2005).

1.2. Histone demethylases

The discovery of several histone demethylases has clearly demonstrated that histone methylation is a reversible and dynamic post-translational modification, contradicting previous beliefs that these modifications were static and irreversible. The first identified histone demethylase is LSD-1 (lysine-specific demethylase), which features the ability to mediate oxidation of N-methylated lysine residues (Shi Y et al, 2007). It directly reverses histone H3K4 or H3K9 modifications by an oxidative demethylation reaction, in which flavin is a cofactor (Metzger E et al, 2005; Shi Y et al 2005). Because lysine residues can be mono-, di- and trimethylated and the LSD-1 family can only remove mono- and dimethyl lysine modifications, the question has been raised whether additional demethylases using a different reaction mechanism exists to remove target trymethylated lysine. In the past few years several JMJDs have been characterized as being capable of catalyzing the removal of all methylation states of H3K4, H3K9, H3K36 and H3K27 (Tab.01).

Demethylases	Targets	Alternative names	Reference
Flavin-dependent			
LSD1	H3K4me1/2, H3K9me1/2 (with AR)	BHC110, AOF2	Shi et al, 2004
FE(II)-2-OG dependent			
JARID1A JARID1B	H3K4me2/3 H3K4me2/3	RBP2 PLU-1	Klose et al, 2007 Seward et al, 2007

JARID1C	H3K4me2/3	SMCX	Iwase et al, 2007
JARID1D	H3K4me2/3	SMCY	Lee et al, 2007
JMJD1A	H3K9me1/2	JHDM2A, TSGA	Yamane et al, 2006
JMJD2A	H3K9me2/3	JHDM3A	Klose et al, 2006
JMJD2B	H3K36me2/3	KIAA0876	Fodor et al, 2006
JMJD2C	H3K9me2/3	GASC1	Cloos et al, 2006
JMJD2D	H3K9me2/3	KIAA0780	Sin et al, 2007
	H3K36me2/3	---	
	H3K9me2/3	---	
JHDM1	H3K36me1/2	FBXL11	Tsukada et al, 2006
UTX	H3K27me1/2/3	---	Agger et al, 2007
JMJD3	H3K27me2/3	---	Agger et al, 2007
JMJD6	H3R2/H4R3me1/2	PTDSR/PSR	Chang et al, 2007

Tab.01: Overview of histone demethylases and their targets showing LSD1 and the family of JmjC domain-containing histone demethylases.

1.2.1. JmjC domain-containing histone demethylases

The largest class of demethylase enzymes containing a Jumonji C (JmjC) domain and catalyzing lysine demethylation of histones through an oxidative reaction that requires iron Fe(II) and α-ketoglutarate (αKG) as co-factors, has been identified recently (Tsukada Y et al, 2006). The JmjC-domain-containing proteins are still a growing family of redox enzymes that catalyze a wide range of oxidation reactions in all living organisms (Clifton IJ et al, 2006). Through these reactions an electron transfer via oxidation (loss of electrons) as well as reduction (gain of electrons) takes place resulting in a change in oxidation number. These reactions are critical steps in the biosynthesis of metabolites, as well as post-translational modification of interacting target proteins involving hydroxylation or demethylation, and DNA/RNA repair of N-methylated nucleic acids (Trewick SC et al, 2005).

By acting as transcription factors, a number of JmjC-domain-containing proteins have been shown to be involved in regulating key processes in mammalian embryogenesis and development. For example, JARID2, part of the subgroup of JmjC-domain containing proteins, has been shown to act as a transcriptional repressor by inhibiting Cyclin D1 during heart and brain development and thereby controlling important steps in cellular proliferation and differentiation in these organs during morphogenesis (Lee Y et al, 2000; Takeuchi T et al, 1999; Toyoda M et al, 2000).

Tsukada et al. have found that JHDM1 (JmjC-domain-containing histone demethylase) can specifically demethylate H3K36me2 and generate a formaldehyde succinate. They were able to identify the JmjC-domain as a novel demethylase signature motif and uncover a protein demethylation mechanism that is conserved from yeast to human (Tsukada Y et al, 2006).

By using a certain biochemical approach, which is able to track formaldehyde production in the chromatography fractions to reflect the histone demethylase activity, Yamane et al. identified JMJD1A, which mediates the demethylation of the repression mark H3K9me2, resulting in gene activation (Yamane K et al, 2006).

In another recent study, a new histone demethylase subfamily, JMJD2, which consists of four members (JMJD2A-D), has been identified (Katho M, 2004). These enzymes are capable of reversing lysine trimethylation, specifically on H3K9me3 and H3K36me3, which leads to gene activation (Whetstine JR et al, 2006).

1.2.2. The demethylase JMJD6

The phosphatidylserine receptor PTDSR, also known as the Jumonji C (JmjC domain containing gene 6 (JmjD6)), is an enzyme with potential arginine demethylase activity. Jumonji C (JmjC)-domain containing proteins are a growing family of redox enzymes that are capable of catalyzing a wide range of oxidation reactions. Arginine methylation occurs on a number of proteins involved in a variety of cellular functions that play a role in cellular differentiation and proliferation during embryogenesis. The tails of histones are known to be mono- and dimethylated on multiple arginine residues where they influence chromatin remodeling and gene expression (Agger K et al, 2007). PTDSR most likely has a function as a nonheme-Fe(II)-2-oxoglutarate-dependent dioxigenase, like other JmjC-domain containing family members as described before (Hahn P et al, 2008).

The human gene JmjD6 was first identified as a putative phosphatidylserine receptor involved in phagocytosis of apoptotic cells (Fadok VA et al, 2000). However, later studies have indicated through failing confirmation, that PTDSR does not directly function in the clearance of apoptotic cells and questioned whether it is a true phosphatidylserine receptor (Tibrewal N et al, 2007). PTDSR was then identified as an arginine demethylase that targets the histone substrates H3 at arginine 2 (H3R2) and

histone H4 at arginine 3 (H4R3) (Agger K et al, 2007). Several groups have reported a nuclear localization of PTDSR, which contradicts the former hypothesis that the protein might function as a transmembrane receptor (Cikala M et al, 2004).

Multiple transcript variants encoding different isoforms have been found for this gene. Chang et al. have also demonstrated in their recent findings, that PTDSR is a JmjC-containing iron- and 2-oxoglutarate-dependent dioxygenase that is a candidate for demethylating histone H3 at arginine 2 (H3R2) and histone H4 at arginine 3 (H4R3) in both biochemical and cell-based assays. PTDSR was shown to demethylate mono- and dimethylated arginine residues, supporting its role as a histone arginine demethylase in the nucleus. However, recent findings of Hahn P et al. (2010) report that PTDSR is not involved in demethylation of the arginine marks as listed above. Instead the group provided evidence that PTDSR may preferentially be associated with RNA/RNA complexes, regulating RNA splicing.

1.3. JMJD6 “knock-out” mice

The importance of this enzyme in embryological development was underlined by experiments of the groups around Böse et al. (2004), Kunasaki et al. (2004) and Li et al. (2003), who found severe anomalies occurring in three impartially generated homozygote JMJD6 -/- mice phenotypes (Fig.05). JMJD6 transcripts could normally be found in different tissues such as brain, eye, spinal cord, liver, kidney and intestines (Li et al, 2003). Delay and defects in terminal differentiation of the kidney, intestine, liver and lung during embryogenesis, brain malformation (midbrain, brainstem cord junction, cerebellum), defective fetal liver erythropoiesis and T-lymphopoiesis, defects in retinal differentiation or complete unilateral or bilateral absence of eyes were detected in the homozygote JMJD6-/- mice by Böse et al. Through RT-PCR, the expression of JMJD6 was detected in all stages of embryonic differentiation, although the expression level varied at different timepoints in the various tissues. Interestingly, the heterozygote JMJD6+/- mice were able to survive and did not show any severe anomalies. These effects seen in the JMJD6- “knock-out” mice raised the question of how this enzyme influences the expression of specific genes that stand in close correlation with tissue differentiation during embryogenesis.

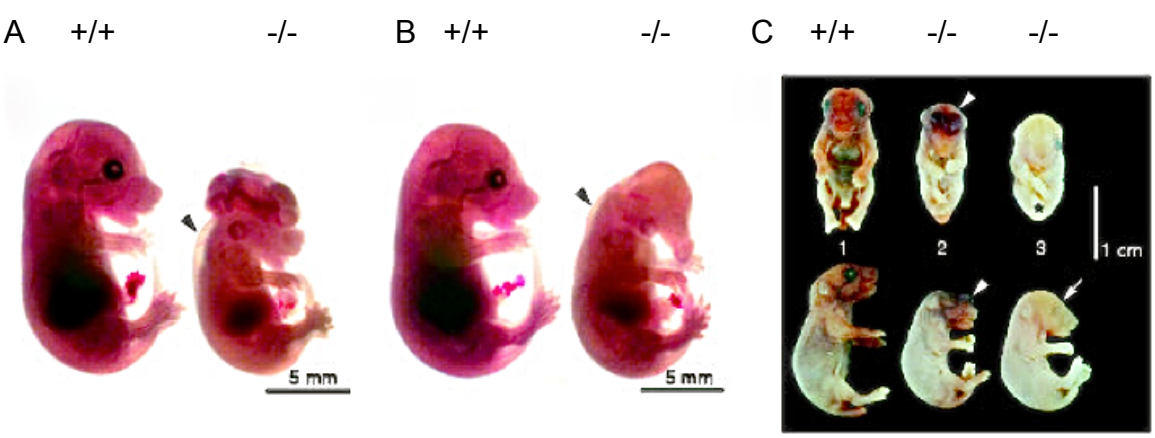

Fig. 05: JMJD6- "knock-out" mice: the homozygote JmjD6-/- mice embryos show major defects in the development of different organs and die perinatally. Embryos at day 15 (A,B) and at the time of birth (C) show for example exencephaly (A) or uni-/bilateral absence of eyes (A,B,C), abnormal head shapes (B), edema (tip of arrow in A,B) and general anemia (3 in C) (Böse et al., 2004)

1.4. Hox genes

Hox genes determine the proper arrangement of embryonic regions along the anterior-posterior body axis in animals during early development. These genes are defined as having a DNA sequence known as the homeobox, which itself is a 180 nucleotide long DNA sequence that encodes a 60 amino-acid-long protein domain known as the homeodomain. Hox genes are arranged in gene clusters on the genome and they show an expression pattern along the anterior-posterior (head to tail) axis that corresponds to the relative location of their genes within the Hox cluster (Fig.06) (Carrol SB, 1995). The protein products of Hox genes are transcription factors that are capable of binding to specific enhancers on the DNA where they either activate or repress genes activation.

Hox genes indirectly control the morphogenesis of specific organs during embryogenesis by activating networks of transcription factors and signaling molecules or by repressing the expression of target genes (Hombria JC et al, 2003). Even a single mutation in the DNA of these genes can have drastic effects on the organism, and so these genes are highly conserved, having changed relatively little over time. However, not all homeodomain proteins are necessarily Hox proteins. Vertebrates feature four Hox gen-clusters on the chromosomes 2, 7, 12 and 17: HoxA, HoxB, HoxC, HoxD.

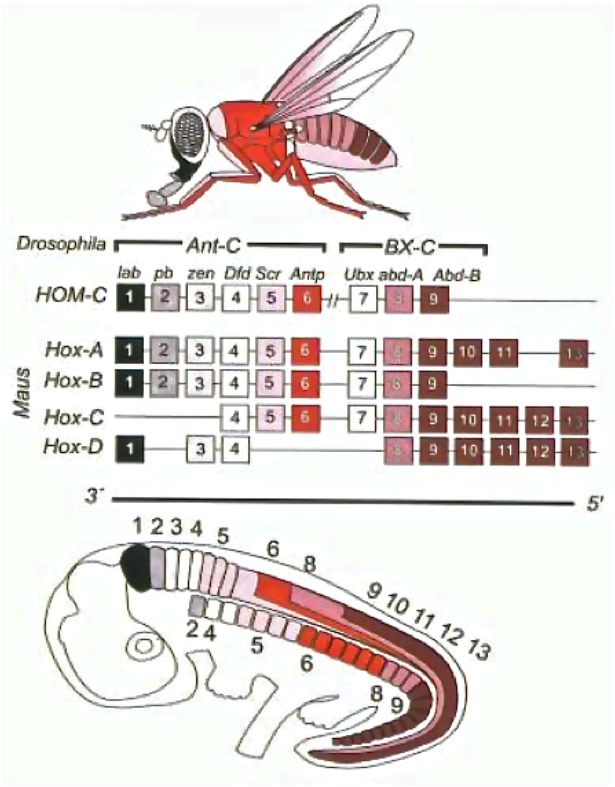

Fig.06: Map of Hox genes.
Comparison between the organization of the Hox genes in Drosophila and mouse. In Drosophila there are nine Hox gene clusters, six of them lying in the Antennapedia-cluster (Ant-C) and three in the Bithorax-Cluster (BX-C). In the mouse there exist four Hox-clusters which originated out of duplication of an ancestral cluster. In the mouse a universal numeral nomenclature is used for the genes, according to the order they are arranged in the cluster (HoxA, HoxB, HoxC, HoxD). The schematic expression domains of the Hox genes are shown in Drosophilia and mouse. The co-linearity between anterior-posterior expression and the organization within the genome is highlighted in the picture by coloring (Picture from Müller and Hassel, 2006)

During development of mammalian limbs, clustered Hox genes are activated in time and space following their genomic topography (Fig.06). This is referred to as co-linearity, leading to both the growth of digits and their morphological identities (Kmita M et al, 2003). Interestingly, the order of the genes on the chromosome is the same as the expression of the genes in the developing embryo, with the first gene being expressed in the anterior end of the developing organism. Montavon and colleagues (2007) have found that the Hox genes located at the 3'-end (early genes) of a cluster were expressed before the ones located at the 5'-end (late genes). This co-linear fashion of activation correlates with the anterior-posterior (AP) polarity of the limb extremities (Drossopoulou G et al, 2000). In insects the Hox genes determine whether an extremity originates at a certain bodysegment or not. Later they regulate which kind of extremity (e.g. antennae, legs, wings etc) is being developed. In vertebrates the Hox genes determine the development of the different vertebrae (cervical-, thoracic- and lumbar vertebra) and ribs.

2. Aim of the thesis

The aim of this project was to identify possible biological targets for PTDSR, which remain unknown so far. Biological targets may be linked to understand its enzymatic activity and may function as cornerstones in further studies. The focus was put on the Hox genes being biological targets for PTDSR because these genes encode for proteins regulating important transcription factors, and therefore have a major effect on epigenetic regulation and development during embryogenesis. PTDSR has been shown to play a role during morphological differentiation. Also, selected neural genes were examined in this study as potential PTDSR targets. In terms of its regulatory mechanisms, we addressed the question whether specific histone methylation residues, such as Histone H1 lysine 26 could be direct targets for PTDSR.

The goals of the thesis are as follows:

1. Identifying possible target genes for PTDSR.
2. Detecting the basic regulatory effect PTDSR has on those genes.
3. Understanding mechanisms underlying the regulation of those genes.

3. Materials and Methods

3.1. Materials

Tab.02: Instruments and supplies

Instrument	Description
Aspiring pipette	5ml (Falcon/ NJ, USA)
Hood	LABCONCO Purifier Class II Biosafety Cabinet (Delta series/ Kansas City, Missouri, USA)
Cell culture plates	96 well, 6 well (Corning Inc., Costar) non- pyrogenic, polystyrene (NY, USA)
ECL kit	Amersham (RPN 2106)
Gel electrophoresis system	(FB-SB-710, Fisher Scientific, USA)
Incubator	Revco Ultima, 37˚C, 71% CO2
Microscope	Nikon TMS (Japan)
Microwave	**(**Kenmore)
Parafilm	pechiney plastic packaging (Mendsha, USA)
PCR tubes	8 strip PCR tubes and Strip caps, clear 125 strips/unit PHOENIX (USA)
Q-PCR machine	Stratagene Mx 3000p, New England Biolabs
Photometer	Eppendorf Biophotometer, 8.5mm Lightcenter height, (Hamburg, Deutschland)
Pipette	with max Volume: 10, 20, 100, 200, 1000µl (RAININ Onsite PM) (Oakland, USA)
Pipette	serological (5, 10, 25, 50ml), (Costar Corning Inc./NY, USA)
Pipette tips	20µl, 250µl, 1000µl pre-sterilized LTS tips, bioclean RAININ Instrument (LLCa Mettler Toledo Company/Oakland, USA)
Polypropylene round bottom tube	14ml, 17x100mm style (FALCON, Becton Dickinson/NJ, USA)
Precast gel	NuPage 4-12% Bis-Tris Gel from INVITROGEN

Refrigerator	**a)** freezer CFC Free (-80˚C) **b)**refrigerator (4˚C) and freezer (-20˚C) (Forma Scientific/Ohio, USA) (Revco/Ohio, USA)
Shaker	Incubator shaker Excella E25R (New Brunswick Scientific)
Sonicator	Ultrasonic Dismembrator 500 (Fisher Scientific, USA)
Speed vac	Speed Vac SC 110 (Savant-Thermo Electron Co., USA)
Stericups	vacuum driven, disposable filtration system, Millipore Durapore 0.22µm (Mass, USA)
Syngene Genius	Quantum BioImaging system (Upland, CA, USA)
Trans-Blot Transfer medium	pure nitrocellulose membrane (0.45µm), (Bio-Rad, Hercules/CA, USA)
UV-cuvettes	UV-cuvette, 500µl (BRAND GmBH)
UV-transilluminator	(Spectroline)

3.1.1. Chemicals, Enzymes, Kits

The chemicals used and pre-made buffers are summarized in Tab.03, enzymes used in Tab.04 and kits used in Tab.05

Tab.03: Chemicals and pre-made buffers:

Abbreviation	Description	Company
Acetyl-CoA	Acetyl-coenzyme A	SIGMA-ALDRICH
Agarose A	Agarose A	BioPioneer Inc.
Amp	Ampicillin sodium salt	Allstar Scientific
β-Mercaptoethanol	β-Mercaptoethanol	SIGMA-ALDRICH
Brilliant Sybr Green	Brilliant Blue G-250	STRATAGENE (CA)
QPCR Master mix		INVITROGEN
DECP-treated water		INVITROGEN
dNTPs	Deoxyribonucleotide triphosphate mix (10mM)	INVITROGEN
DTT	Dithiothreitol	Fisher scientific
EDTA	Ethylene diamine tetraacetic	Allstar Scientific

EthBr	acid Ethidium bromide solution	 INVITROGEN
Isopropanol	(10mg/ml)	
1 kb DNA ladder	2-Propanol	Fisher Scientific
Loading buffer	1kb DNA ladder	NEB
MeOH	6x loading dye solution	NEB
MgCl2	Methanol	NEB
NaCl	Magnesium chloride	Fisher Scientific
NaH2PO4	Sodium chloride	TEKNOVA
	Sodium phosphate,	Fisher Scientific
NaOH	monobasic	TEKNOVA
Nonfat dry milk	Sodium hydroxide	TEKNOVA
Protease inhibitor	Carnation Nestle	Nestle
cocktail		Fisher Scientific
protein A-sepharose		young America (MN, USA)
beads	Protein beads for ChIP	Complete, ROCHE
Protein marker Seablue		
	Protein marker	provided by the Rosenfeld
RA		laboratory, UCSD
20% SDS	Retinoic acid	INVITROGEN
TE buffer	Sodium dodecylsulfate	INVITROGEN
Tris-CL 7,8		SIGMA-ALDRICH
	2-Amino-2(hydroxymethyl)-	TEKNOVA
Triton-X 100	1,3-propanediol	
Tween 20		Fisher Scientific
		Fisher Scientific

Tab.04 Enzymes used:

Enzyme	Company
CIP (Calf Intestinal Phosphatase)	New England Biolabs
DNA Polymerase	INVITROGEN
DNaseI	INVITROGEN
EcoRI	New England Biolabs
Hpa1	New England Biolabs
Lysozyme	SIGMA-ALDRICH
RNaseOUT	INVITROGEN

SuperScript III RT	INVITROGEN
T4-DNA-Ligase	ROCHE
Trypsin	SIGMA-ALDRICH
Xho1	New England Biolabs
Not1	New England Biolabs
BamH1	New England Biolabs

Tab.05 Antibodies used for ChIP

Antibody		Company
Histone H1 (tri methyl K26) antibody	cat# ab17347	ABCAM
Histone H1 (di methyl K26) antibody	cat# ab20652	ABCAM
L3MBTL1 antibody - ChIP Grade	cat# ab51880	ABCAM
ANTI-FLAG	cat# F1804	SIGMA-ALDRICH

Tab.06:Vector used for ChIP

p3xFLAG-CMV™-10	cat# E4401	SIGMA-ALDRICH

Tab.07: Primers used to detect mRNA expression levels of PTDSR (actin was taken as control)

actin(mRNA)5	accaactgggacgacatggagaaa
actin(mRNA)3	tagcacagcctggatagcaacgta
PTDSR(mRNA)5	ctgaattcaaacccctggaa
PTDSR(mRNA)3	taccgtcttgtgccatacc

Tab.08: Primers used for ChIP to detect binding of PTDSR on promoter regions of Hox genes

ChIP Hox gene oligos	Oligo sequence (5'→3')
HoxA1 5'	ccctcttcccttctcacctc
HoxA1 3'	gaagagcaaaagctgcgttc
HoxA2 5'	aattgtcattgggcagaagc
HoxA2 3'	gccccctcagagaaaaagtt
HoxA3 3'	taagcgacaccccaagtttc
HoxA3 5'	gtctggagttgggggatttt
HoxA4 5'	aggagcggctcgaacttt
HoxA4 3'	atttttctcgcgttgtcgtt
HoxA5 5'	tcggaagctgggcgatgag
HoxA5 3'	gtgcactaataggggagttggg
HoxA9 5'	gggagacgggagagtacagagac
HoxA9 3'	cgtccagcagaacaataacgcg

HoxB2 5’	cgtggtcctctggtgttttt
HoxB2 3’	ggggagatttcggtctctct
HoxB3 5’	gagggactaggggaggtcag
HoxB3 3’	aaaaagcccaccagttttca
HoxB4 5’	ccccgcaggagccctatgta
HoxB4 3’	gtaggtaatcgctctgtgaata
HoxB5 5’	tgtttctccccttctcctt
HoxB5 3’	gggaatcacgtgcttttgtt
HoxB6 5’	ccaaatctcacccttctca
HoxB6 3’	atcgctggattcaaccactc
HoxB7 5’	attcaatccctgcgtttgtc
HoxB7 3’	aattgtgtggcgttggattt
HoxB8 5’	tgtcggcttcgagatcttct
HoxB8 3’	aggctatagttgggggctgt
HoxB13 5’	ttttcgcagtttctgccttt
HoxB13 3’	ttttaaatcgctcccagctc
HoxC4 5’	ggggatgctccctctatga
HoxC4 3’	catggatggaatccacatga
HoxC5 5’	ggctcccttatttgggaaga
HoxC5 3’	ggctacgtaggagctcatgg
HoxC10 5’	tggataaacaaaccccactctt
HoxC10 3’	ccaatgggatttgaaaatgg
HoxD1 5’	gtccagtcctgcctttctcc
HoxD1 3’	agccaagttagccaaagcag
HoxD3 5’	ggttaggctgtttggtgcaggtg
HoxD3 3’	cataggtcagctccctggtctc
HoxD4 5’	aaggttggcaaaatcagtgg
HoxD4 3’	caagtttatcaccgggttgg
HoxD8 5’	acacctcttgtccacgttcc
HoxD8 3’	taaaggggcccataaagac
HoxD9 5’	ctccgatctgctccatccg
HoxD9 3’	ctcgcctctctccctactca
HoxD10 5’	tctcattggcttggttgtca
HoxD10 3’	gcaggcactgatcaaggaat
HoxD11 5’	cggaaagagccaagtcactc
HoxD11 3’	ggtgtgagggtgtgaggttc
HoxD12 5’	ggaaacccgcagacagttag
HoxD12 3’	caaccgggaataagaggaggaca
HoxD13 5’	tcctcttctgccgttgtagc

HoxD13 3’	gatgacttgagcgcattctg

Tab.09 Primers used for RT- qPCR to check Hox gene expression after microarray

QPCR Hox gene oligos	Oligo Sequence(5'→3')	Tm
HoxA1 5'	5'-CCAGCCACCAAGAAGCCTGT-3'	60.3
HoxA1 3'	5'-CCAGTTCCGTGAGCTGCTTG-3'	58.8
HoxA2 5'	5'-ACAGCGAAGGGAAATGTAAAAGC-3'	56.1
HoxA2 3'	5'-GGGCCCCAGAGACGCTAA-3'	59.8
HoxA3 5'	5'-TGCAAAAAGCGACCTACTACGA-3'	56.5
HoxA3 3'	5'-CGTCGGCGCCCAAAG-3'	57.7
HoxA4 5'	5'-CGTGGTGTACCCCTGGATGA-3'	58.9
HoxA4 3'	5'-AAGACCTGCTGCCGGGTGTA-3'	61.3
HoxA5 5'	5'-TCTACCCCTGGATGCGCAAG-3'	59.5
HoxA5 3'	5'-AATCCTCCTTCTGCGGGTCA-3'	58.5
HoxA6 5'	5'-TGGATGCAGCGGATGAACTC-3'	57.6
HoxA6 3'	5'-CCGTGTCAGGTAGCGGTTGA-3'	59.5
HoxA7 5'	5'-TCTGCAGTGACCTCGCCAAA-3'	59.3
HoxA7 3'	5'-AGCGTCTGGTAGCGCGTGTA-3'	61.1
HoxA9 5'	5'-ACGTGGACTCGTTCCTGCTG-3'	59.7
HoxA9 3'	5'-AGGTTTAATGCCATAAGGCCG-3'	55.5
HoxA10 5'	5'-CCTTCCGAGAGCAGCAAAGC-3'	58.8
HoxA10 3'	5'-CAGCGCTTCTTCCGACCACT-3'	60
HoxA11 5'	5'-ACAGGCTTTCGACCAGTTTTTC-3'	55.9
HoxA11 3'	5'-CCTTCTCGGCGCTCTTGTC-3'	58.4
HoxA13 5'	5'-ACTCTGCCCGACGTGGTCTC-3'	61.5
HoxA13 3'	5'-TTCGTGGCGTATTCCCGTTC-3'	57.7
HoxB1 5'	5'-CTCCTCTCCGAGGACAAGGAA-3'	58
HoxB1 3'	5'-CTGTCTTGGGTGGGTTTCTCTTAA-3'	56.7
HoxB2 5'	5'-CAATCCGCCACGTCTCCTTC-3'	58.3
HoxB2 3'	5'-CAGCAGCTGCGTGTTGGTGT-3'	61.2
HoxB3 5'	5'-GCACCAACTCCACCCTCACC-3'	60.8
HoxB3 3'	5'-GCCACCACAGCCCTCTGC-3'	62.1
HoxB4 5'	5'-CTACCCCTGGATGCGCAAAG-3'	58.5
HoxB4 3'	5'-TCCAGCTCCAAGACCTGCTG-3'	59.5

HoxB5 5'	5'-TCCGCAAATATTCCCCTGGA-3'	56.2
HoxB5 3'	5'-CGGGTCAGGTAGCGGTTGAA-3'	59.6
HoxB6 5'	5'-CTCCGGTCTACCCGTGGATG-3'	59.4
HoxB6 3'	5'-CCGCGTCAGGTAGCGATTGT-3'	60
HoxB7 5'	5'-GACTTGGCGGCGGAGAGTAA-3'	59.5
HoxB7 3'	5'-CAGGGTCTGGTAGCGGGTGT-3'	61.6
HoxB8 5'	5'-AACTCACTGTTCTCCAAATACAAAACC-3'	55.8
HoxB8 3'	5'-GACGGCCCGTGGTAGAACT-3'	59.5
HoxB9 5'	5'-TTTGCGAAGGAAGCGAGGAC-3'	57.9
HoxB9 3'	5'-AGCTCCAGCGTCTGGTATTTGG-3'	59.3
HoxB13 5'	5'-CCACTGGCTGCTGGACTGTT-3'	60.2
HoxB13 3'	5'-TATGACTGGGCCAGGTTCTTTG-3'	57.1
HoxC4 5'	5'-CGCCAGCAAGCAACCCATAG-3'	59.2
HoxC4 3'	5'-TGCTGCCGGGTATAGGCTGT-3'	61.2
HoxC5 5'	5'-AGGTGCAGGCATCCAGGTACT-3'	60.7
HoxC5 3'	5'-GGGTTGGCAGCCATGTCTAC-3'	58.5
HoxC6 5'	5'-TCAAACGTGGACCTGAAAGTCA-3'	56.5
HoxC6 3'	5'-GGGAAAAGGGCCTGTAGACAA-3'	57.1
HoxC8 5'	5'-AGCGAAGGACAAGGCCACTT-3'	59.4
HoxC8 3'	5'-GGCTGTAAGTTTGCCGTCCA-3'	58
HoxC9 5'	5'-AGGAGAAGGCCGACCTGGAC-3'	61.4
HoxC9 3'	5'-TTCCAGCGTCTGGTACTTGGTG-3'	59.2
HoxC10 5'	5'-CGACTCCAGCCCAGACACCT-3'	61.5
HoxC10 3'	5'-GCGCTCTCGCGTCAAATACA-3'	58.1
HoxC11 5'	5'-GTGAAGGGAAGTGTCTGATGCA-3'	57.2
HoxC11 3'	5'-AATCCGAGCAGCAAGACATTG-3'	55.8
HoxC12 5'	5'-TAATCTCCTGAATCCCGGGTTT-3'	55.7
HoxC12 3'	5'-TGGGTAGGACAGCGAAGGC-3'	59.7
HoxC13 5'	5'-TCATCCCCGTCGAAGGCTAC-3'	58.9
HoxC13 3'	5'-TGTAGGGCACGCGTTTCTTG-3'	58.2
HoxD1 5'	5'-CCTTCAGCACGTTCGAGTGG-3'	58.4
HoxD1 3'	5'-CGCCGGGCTCGAGTTAAGTA-3'	59.2
HoxD3 5'	5'-CCATAAATCAGCCGCAAGGAT-3'	55.5

HoxD3 3'	5'-GATCGGTCTCAGACTTACCTTTGG-3'	56.9
HoxD4 5'	5'-CCGTGGTCTACCCCTGGATG-3'	59.6
HoxD4 3'	5'-TAGGACTTGCTGCCGGGTGT-3'	61.3
HoxD8 5'	5'-TATTGGCGAGGACCCAGACC-3'	59
HoxD8 3'	5'-GCTAGGGCGTGGGAAACCTC-3'	60.5
HoxD9 5'	5'-GGCTGTTCGCTGAAGGAGGA-3'	59.6
HoxD9 3'	5'-TCTCCAGCTCAAGCGTCTGGT-3'	60.6
HoxD10 5'	5'-ATAAGCGCAACAAACTCATTTCG-3'	54.5
HoxD10 3'	5'-ATATCGAGGGACGGGAACCT-3'	57.5
HoxD11 5'	5'-GAGAAGAGCAGCAGCGCAGT-3'	60.3
HoxD11 3'	5'-TGCCGGTCAGTGAGGTTGAG-3'	59.6
HoxD12 5'	5'-TGTGTGAGCGCAGTCTCTACAGA-3'	59.8
HoxD12 3'	5'-CGGCCTCAGGTTGGAGAAG-3'	58
HoxD13 5'	5'-CTGGGCTACGGCTACCACTTC-3'	59.7
HoxD13 3'	5'-GCGATGACTTGAGCGCATT-3'	56.3

5’ being forward primer, 3’ being reverse primer, Tm: Primer melting temperature

3.1.2. Genomic DNA

The PTDSR genomic cDNA sequence was derived from the UCSC genomic browser and kindly provided by Wen Liu from the laboratory of Michael Geoff Rosenfeld University of California San Diego (UCSD Center for Molecular Biology). The concentration was 10ng/µl.

3.1.3. Media

Tab.10: Media used

Cell culture medium	Company
DMEM+Glutamax, low glucose 1x, 10% SFCS, no antibiotics	GIBCO 10561
MEMα+Glutamax, Alpha Medium 1x, 10%SFCS, no antibiotics	GIBCO 32571
0.25% Trypsin-EDTA 1x	GIBCO 25200
Lipofectamine 2000	INVITROGEN
Opti-MEM	GIBCO

SOC- Medium used in virus transfection:
2% Bacto-Trypton
0.5% yeast extract,
0.5% NaCl,
2.5mM KCl,
10mM $MgCl_2$,
20mM glucose, pH 7,0

The agar plates used for seeding competent cells used for cloning and the LB medium for the bacteria culture were prepared as follows:

Luria-Bertani medium (LB medium)

		End conc.
Yeast extract		10g
Pepton	EMD premix	10g
NaCl		5g
ddH2O		ad 1000ml

- autoclave at 121°C for 1h

Luria-Bertani agar (LB agar)

		End conc.
Yeast extract		10g
Pepton	EMD premix	10g
NaCl		5g
Agar-agar		12g
ddH2O		ad 1000ml

- autoclave at 121°C for 1h

3.1.4. Kits

Tab.11: Kits used

Kit	Company
· Lipofectamine 2000 formulation	INVITROGEN
· Plasmid purification Midi Prep	QIAGEN
· QIAGEN quick spin Kit	QIAGEN
· RNeasy kit	QIAGEN
· SuperScript III First-Strand Synthesis System for RT-PCR (Cat.No: 18080-051)	INVITROGEN
· Taq DNA Polymerase	INVITROGEN
· Rapid DNA ligation Kit	ROCHE

3.1.5. Solutions and buffers

Solutions for ChIP:

Crosslinking mix

-11% formaldehyde
-100mM NaCl
-0.5mM EGTA
-50mM HEPES, pH 8.0

Lysis buffer

- 1% SDS
- 10mM EDTA, pH 8.0
- 50mM Tris-HCl, pH 8.0, with protease inhibitor cocktail, which was prepared by dissolving one protease inhibitor tablet (complete, ROCHE) in 1ml water.

Dilution buffer

- 1% Triton X-100
- 150mM NaCl
- 2mM EDTA, pH 8.0
- 20mM Tris-HCl, pH 8.0,with protease inhibitor

Washing buffer

- 1% Triton X-100
- 0.1% SDS
- 150mM NaCl
- 2mM EDTA, pH 8.0
- 20mM Tris-HCl, pH 8.0, with protease inhibitor

Final wash

- 1% Triton X-100
- 0.1% SDS
- 500mM NaCl
- 2mM EDTA, pH 8.0
- 20mM Tris-HCl, pH 8.0, with protease inhibitor

Elution

- 1% SDS
- 100 mM $NaHCO_3$

Buffers for Western blot:

Lysis buffer:

- 0.15 M NaCl
- 5 mM EDTA, pH 8
- 1% Triton X100
- mM Tris-Cl, pH 7.4
- Just before using add: 1:1000 5 M DTT
- 1:1000 100 mM PMSF in isopropanol
- 1:1000 5 M e-aminocaproic acid

10x Running buffer:

- 30.3 g Trizma base (= 0.25 M)
- 144 g Glycine (= 1.92 M)
- SDS (= 1%)--add last

10x Blotting buffer:

- 30.3 g Trizma base (= 0.25 M)
- 144 g glycine (= 1.92 M)
- The pH should be 8.3!
- The 1x blotting buffer is obtained by mixing Methanol and 10x Blotting buffer in the ratio 2:1 and then filled up with H2O.

Blocking buffer (TBST mix):

- 35,064g NaCl
- Tris-Cl pH 8,0
- Tween 20
- The mix is kept at 4°C to prevent bacterial contamination.
- 5% dry milk + TBST = 2.5g milk dissolving in 50ml TBST

3.1.6. HEK293T and NTera2 cell lines

Human embryonic kidney cells, also known as HEK cells, HEK 293, or just 293T cells, are a cell line originally derived from an embryonic human kidney. 293T cells have been grown in tissue culture for many years and are widely used in cell biology research. They are relatively easy to grow and transfect at high efficiency. For this project they were a convenient model to work with, being easy to culture and transfect, and so can be used in experiments aimed at gene functions and not the behavior of the cell itself.

The other cell line used in the experiments was NTera2/D1 (NT2). The NT2 cell line has properties similar to those of progenitor cells in the central nervous system (CNS).

These neural-like precursor cells can differentiate into all three major lineages (neurons, astrocytes, and oligodendrocytes) after exposure to retinoic acid (RA). As such, they are widely used as a model system for studying neurogenesis (Coyle DE et al., 2011).

3.1.7. Cell culture

The NTera2 cells (neural cell line) were plated at a density of 10,000–15,000 cells per cm^2 at 37°C in 5% CO_2 and maintained in Dulbecco's modified Eagle's medium (DMEM)+Glutamax (GIBCO), low glucose 1x, supplemented with 10% fetal bovine serum (FBS) and no antibiotics. The cells were fed twice a week and split 1:4 when confluent by mechanical scraping.
Then cells were cultured in $10cm^2$ plates with cell-density of $1x10^6$ in 10ml medium for virus infection.

3.1.8. Oligonucleotide design

For the generation of the shRNA-containing lentivector, oligonucleotides had to be designed, containing the right insert after hybridization and also the matching ends for ligation into the vector.
Firstly the design creation of the siRNA to knock down the gene of interest was selected according to http://www.rockefeller.edu/labheads/tuschl/sirna.html.
With this siRNA-sequence the sense- and antisense-sequence of
the oligos for creating PTDSRshRNA (short hairpin RNA) stem loops for LentiLox3.7 were designed according to this website:
http://jura.wi.mit.edu/bioc/siRNAext/home.php

Tab.12: Oligonucleotides, containing cohesive Xho and Hpa1 (restriction enzymes) sites used in shRNA (human)

Forward primer: tGCTATTACCTGGTTTAATGttcaagagaCATTAAACCAGGTAATAGCttttttC
Reverse primer: TCGAaaaaaaGCTATTACCTGGTTTAATGtctcttgaaCATTAAACCAGGTAATAGCa

3.2. Methods

3.2.1. siRNA transfection

Transfection was performed using Lipofectamine 2000 (Invitrogen Inc.) formulation for the transfection of nucleic acids (DNA and RNA) into eukaryotic cells. Lipofectamine 2000 was first gently mixed with Opti-MEM reduced serum medium and then incubated at room temperature for 5 minutes. The Opti-MEM-Lipofectamine 2000 solution was then mixed with either control or PTDSR siRNA oligomers diluted in Opti-MEM reduced serum medium and incubated for 20 min at room temperature before adding to Ntera2 cells. The NTera2 cells were 30-50% confluent in 6-well plates at the time of transfection. Cells were treated with retinoid acid (RA) (10^{-6}M) 48 hours after siRNA transfection to activate HOX gene expression (Ogura T. 1995, Duester G. 2008). Therefore, this experiment included the following conditions:

- Control siRNA
- Control siRNA + RA
- PTDSR siRNA
- PTDSR siRNA + RA

3.2.2. Isolation of total RNA from cells

Isolation of total RNA from NTera2 cells was performed by using the RNeasy Mini Kit from QIAGEN. The cells were disrupted and homogenized at a density of $2.5x10^6$ in $60mm^2$ plates in 600μl of RLT buffer, containing 1% of β-mercaptoethanol for 15 min. One volume of 70% ethanol is then added to the lysate, creating conditions that promote selective binding of RNA to the RNeasy membrane. The sample is then applied to the RNeasy Mini spin column. Total RNA binds to the membrane, contaminants are efficiently washed away, and high-quality RNA is eluted in RNase-free water. All bind-, wash-, and elution-steps are performed by centrifugation in a microcentrifuge (10,000 rpm).

3.2.3. Measuring RNA concentration

The concentration of the RNA was determined by measuring the absorbance at 260nm (A260) in a spectrophotometer. To ensure significance, readings should be greater than

0.15. An absorbance of 1 unit at 260nm corresponds to 40µg of RNA per ml (A260=1=40µg/ml). This relation is valid only for measurements in water, using RNAse-free cuvettes.
Therefor 2µl of eluted RNA samples were diluted 50 times with H2O and then measured by using Eppendorf BioPhotometer (Hamburg/Germany) with 8.5mm light center height. The final concentration of RNA was calculated based on A260. RNA concentration = A260*40*50.

3.2.4. cDNA synthesis

For the cDNA synthesis from purified RNA of NTera2 cells, the SuperScript III First-Strand Synthesis System for RT-PCR from Invitrogen, Inc (Catalog No: 18080-051) was used. The procedure is described below.

RNA/Primer mixture

- Up to 5µg total RNA
- 10mM dNTP mix
- DEPC-treated water adding up to 10 µl

cDNA synthesis mix

- 10x RT buffer
- 25mM MgCl2
- 0.1 M DTT
- RNaseOUT (40U/µl)
- SuperscriptIII RT (200U/µl)

First, RNA was treated with DNase to eliminate remaining DNA. Therefor, 5.2 µl RNA was incubated with 1 µl DNase I, 0.8 µl 10 x DNase I buffer and 1 µl RNase out (15 minutes, RT). DNase was inactivated by adding 1 µl EDTA (25 µM) and incubated (65°C, 10 minutes). First strand cDNA synthesis was achieved by incubating the RNA with 2 µl dNTPs (10 mM) and 1 µl random hexamers (300 nM) (65°C, 5 minutes). After a quick chill on ice for at least 1 minute, 2 µl 10 x first strand buffer, 2 µl DTT(0.1M) and 1 µl RNase-out (40U/µl) were added and the mixture was incubated (10 minutes at 50°C). cDNA synthesis was started by adding 1 µl Superscript II and incubation (50 minutes at 25°C). Reaction was stopped through incubation (5 minutes at 85°C). cDNA was stored at -20°C. As a control, no RT samples (RNA samples which undergone DNase treatment but no reverse transcription) were generated similarly and used as a negative control in real time RT PCR analysis.
After collecting the reactions through brief centrifugation 1µl of RNase H is added to each tube and incubated at 37˚C for 20 minutes. The cDNA synthesis reaction can now be stored at -20˚C or used for PCR immediately.

3.2.5. Agarose gel electrophoresis

To determine the size of DNA-fragments, a 2% agarose-gel electrophoresis was used, which separates the DNA molecules by size using electric current. The separation of DNA was done in a horizontal electrophoresis system (FB-SB-710, Fisher Scientific). Agarose solution in 0.5X TBE buffer was prepared by heating in a microwave and cooled to about 55˚C. Ethidium bromide was added at a final concentration $2x10^{-4}$ μg/μl before the gel was cast in a gel-slide with a 12 pocket comb within the used horizontal electrophoresis system. The solid gel was then placed into the electrophoresis chamber filled with 0.5X TBE buffer and DNA samples were pipetted into the gel pockets as a 5:1 mix with 6x loading buffer. For analysis of the DNA fragment sizes, one DNA ladder was loaded per gel. The agarose gel electrophoresis was run for 60 min at a voltage of 150V. The documentation of the gel was done under UV light exposure via a Syngene Genius gel documentation station (Quantum BioImaging system).

3.3. Microarray analysis

NTera2 cells were infected with either control or PTDSR shRNA lentivirus followed by treatment with or without RA. shRNA knock-down efficiency was determined by immunoblotting and RT-qPCR. Total RNA was isolated from NTera2 cells using RNeasy Mini Kit (Qiagen) with DNase I in column digestion. The microarray experiments and data normalization were performed at the UCSD BIOGEM laboratory. RNA quality was assessed using an Agilent Bioanalyzer. Total RNA (250ng) was labelled with biotin using the Ambion Illumina TotalPrep RNA Amplification kit. cRNA (1,500ng) was hybridized to the Sentrix Human-6 v2 expression BeadChIP from Illumina for 18 hours at 58˚C and then stained with Steptavidin-Cy3. Slides were scanned using the Illumina BeadArray Reader scanner and raw data extracted with the Illumina BeadStudio software. The data were then processed according to Illumina protocols and normalized using the multi-loess method ‘mloess’ as described previously (Sâsîk R. et al, 2004). The differential expression analysis was performed by using the SAM (significance analysis of microarrays) method (Tusher, VG et al, 2001) implemented in MeV/TM (Saeed AI et al, 2006) and in the R package ‘siggenes’ (Schwende H. et al, 2008) and the FDR (False Discovery Rate) was sequentially set up

at distinct values lower than 0.25. The gene ontology analysis was done with DAVID/EASE tools (Huang DW et al, 2009) (http:// david.abcc.ncifcrf.gov/).

3.4. Chromatin immunoprecipitation (ChIP)

To detect a specific regulatory protein/transcription factor binding to certain genomic DNA regions, ChIP assays were performed (Fig.07). This assay, where protein-DNA complexes are crosslinked, immunoprecipitated, purified, and amplified, is used for gene- and promoter-specific analysis of known targets or for the identification of new target sequences. In the last step, when the crosslinks are reversed, the purified DNA reveals the transcription factor binding and thereby its targets. This experimental procedure was used to study whether PTDSR targets to Hox genes.

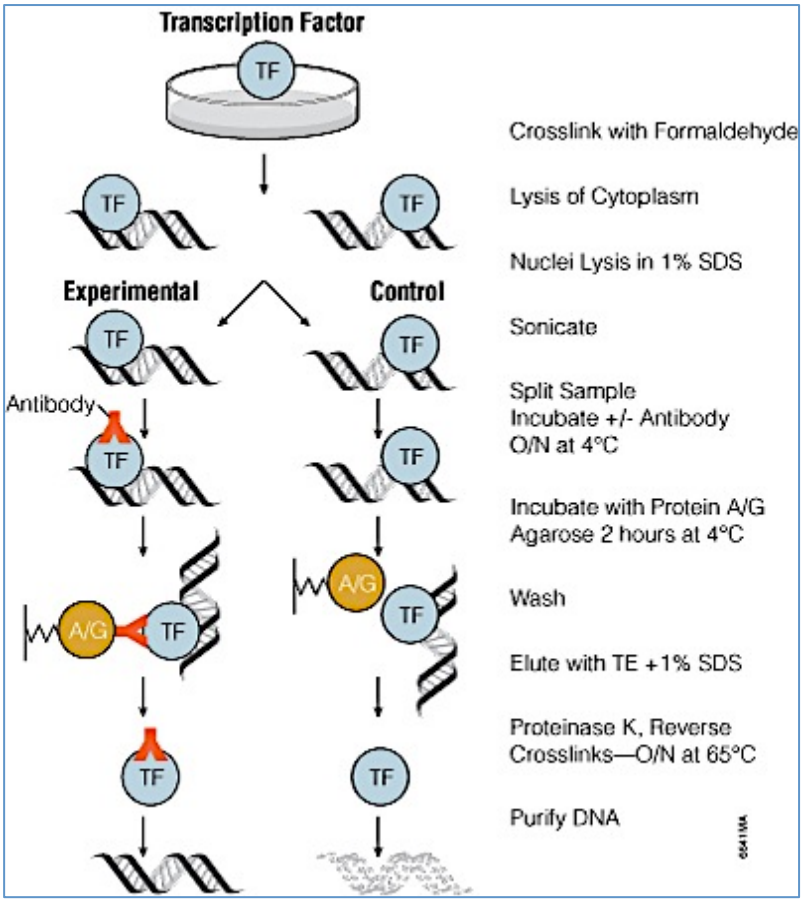

Fig.07:ChIP. Chromatin immunoprecipitation using antibodies
TF=Transcription Factor,A/G= protein beads, O/N=over night (www.promega.com)

3.4.1. Formaldehyde crosslinking

The NTera2 cells were seeded on 100mm plates and grown up to 98% confluence. To crosslink the DNA-binding proteins to the DNA, cells were treated with 1% Formaldehyde/PBS fixation solution and incubated for 10 minutes at RT. After washing the cells twice with PBS, 1ml stop solution (100mM Tris.HCl, pH 9.4, 10mM DTT) was added to each plate. Cell were then collected with a scraper into 1.5ml eppendorf tubes, washed with ice-cold PBS once again, centrifuge down and resuspended in 300µl lysis buffer (1% SDS, 10mM EDTA, 50mM Tris.HCl, pH 8.1 and protease inhibitor cocktail (Roche)).

3.4.2. Preparation of the cell lysate for immunoprecipitation

The crosslinked chromatin was sheared by sonication (4 times 10sec) to reduce the average DNA fragment size to 0.2-1 Kb in length. To determine the DNA fragment size after sonication, 5µl of samples were taken and heated in a boiling water bath for 5min before performing agarose gel electrophoresis. After spinning down the samples at 14,000rpm for 10min, the supernatant was diluted with dilution buffer (1% Triton X-100, 2mM EDTA, 150mM NaCl, 20mM Tris.HCl, pH8.1and protease inhibitor cocktail) for immunoprecipitation. 5µl of undiluted supernatant was kept as input.

3.4.3. Immunoprecipitation of the target protein

Primary antibodies for ChIP (Tab.05) were added to the diluted lysates and incubated at 4˚C on rotator over night. To capture the immune complexes, 40µl protein A-sepharose beads were added to the tubes and incubated for 6 hours at 4˚C.

3.4.4. Isolation of DNA associated with the immunoprecipitated protein

To remove DNA and proteins nonspecifically associated with the protein A-sepharose, the mixture was washed once with TSEI buffer (0.1% SDS, 1% Triton X-100, 2mM EDTA, 20mM Tris.HCl pH 8.1, 150mM NaCl), once with TSEII buffer (0.1% SDS, 1% Triton X-100, 2mM EDTA, 20mM Tris.HCl pH 8.1, 500mM NaCl) and rinsed twice with TE buffer. The DNA-protein complex was de-crosslinked with 300µl of TE/SDS Buffer (1% SDS) overnight at 65°C.

3.4.5. Analysis of DNA associated with the immunoprecipitated protein

The DNA was purified using the QIAquick spin Kit (QIAGEN) following the manufacturer protocol. Briefly, 5 volumes of Buffer PB were added to the ChIP DNA samples and placed a QIAquick spin column. After DNA binding- and washing-steps the DNA was eluted by adding 60 µl Buffer EB (10 mM Tris·Cl, pH 8.5) or H2O to the center of the QIAquick membrane. The eluted DNA samples were analyzed by RT-qPCR using the primers listed in Tab.09.

3.4.6. Quantitative PCR/ realtime PCR (qPCR)

Following the mRNA extraction and ChIP, RT-qPCR was performed to detect the binding of protein of interest to targeted genomic loci by using Mx3000P machine (Stratagene). DNA samples were diluted 4 times with H2O prior to RT-qPCR set up as following.

RT-qPCR mixture:

Primers (forward and reverse strand):	1µl (concentration: 12.5 uM)
Brilliant Sybr Green QPCR mix (2X):	5µl
DNA sample:	4µl

4µl of DNA sample and then 6µl of the primer/sybr green mix were loaded to the RT-qPCR plates (96-well format). The plate was then centrifuged briefly to collect all the samples to the bottom of the wells. MxPro software supplied by Stratagene was used to analyze all the RT-qPCR data.

Thermal profile setup of the RT-qPCR:

1) 95˚C	10min	
2) 95˚C	20sec	
3) 55˚C	20sec	
4) 70˚C	30sec	repeat step 2 to 4 for 45 cycles
5) 95˚C	1min	
6) 55˚C	30sec	
7) 95˚C	30sec	

3.5. Virus transfection

In order to induce RNA interference into cell types, tissues and organisms, a virus system is commonly used as the vector. Through this vector it is possible to infect and efficiently silence proteins in cells by inducing the siRNA.

For the virus production in this thesis work, the LentiLox 3.7 (pLL3.7) was used. LentiLox 3.7 is a lentiviral vector designed for stably inducing siRNA (small interfering RNA) in a wide range of cell types, tissues and organisms (http://web.mit.edu/jacks-lab/protocols/pll37.htm).

3.5.1. Cloning

Tab.13: shRNA Oligos (nuleotides sequences targeting to PTDSR or a scramble sequence) Design:

PTDSR(shRNA)1-5	tGAACTGGGATTCACATCGAttcaagagaTCGATGTGAATCCCAGTTCttttttC
PTDSR(shRNA)1-3	TCGAGaaaaaaGAACTGGGATTCACATCGAtctcttgaaTCGATGTGAATCCCAGTTCa
PTDSR(shRNA)2-5	tGGATAACGATGGCTACTCAttcaagagaTGAGTAGCCATCGTTATCCttttttC
PTDSR(shRNA)2-3	TCGAGaaaaaaGGATAACGATGGCTACTCAtctcttgaaTGAGTAGCCATCGTTATCCa
PTDSR(shRNA)3-5	tGACCAAAGTTATCAAGGAAttcaagagaTTCCTTGATAACTTTGGTCttttttC
PTDSR(shRNA)3-3	TCGAGaaaaaaGACCAAAGTTATCAAGGAAtctcttgaaTTCCTTGATAACTTTGGTCa
PTDSR(shRNA)4-5	tGGACCCGGCACAACTACTAttcaagagaTAGTAGTTGTGCCGGGTCCttttttC
PTDSR(shRNA)4-3	TCGAGaaaaaaGGACCCGGCACAACTACTAtctcttgaaTAGTAGTTGTGCCGGGTCCa
Control(shRNA)1-5	tATGCACGTGCACATATCCCttcaagagaGGGATATGTGCACGTGCATttttttC
Control(shRNA)1-3	TCGAGaaaaaaATGCACGTGCACATATCCCtctcttgaaGGGATATGTGCACGTGCATa

The oligo aiming to knock-down target gene was designed using the free tool from http://jura.wi.mit.edu/bioc/siRNAext/home.php or http://www.dharmacon.com/DesignCenter/DesignCenterPage.aspx.

After choosing the targeting sequences, the RNAi stem loop for pLL3.7 was created following the outline below (sequence pair 1 was used as an example).

1. Add sequences for restriction sites and loop

GAACTGGGATTCACATCGA

2. Add T to the beginning of G(N18) to recreate -1 in U6 promoter

*T*GAACTGGGATTCACATCGA

3. Add loop sequence to end - TTCAAGAGA

*T*GAACTGGGATTCACATCGA*TTCAAGAGA*

4. Add reverse complement of G(N18) to end - i.e. GAT then added ATC

*T*GAACTGGGATTCACATCGA*TTCAAGAGA*TCGATGTGAATCCCAGTTC

5. Add terminator sequence - 6 Ts

*T*GAACTGGGATTCACATCGA*TTCAAGAGA*TCGATGTGAATCCCAGTTC*TTTTTT*

6. Create antisense strand

*T*GAACTGGGATTCACATCGA*TTCAAGAGA*TCGATGTGAATCCCAGTTC

TTTTTT

ACTTGACCCTAAGTGTAGCTAAGTTCTCTAGCTACACTTAGGGTCAAGAAAAAA

7. Add sticky end for Xho site

*T*GAACTGGGATTCACATCGA*TTCAAGAGA*TCGATGTGAATCCCAGTTC

TTTTTTC

ACTTGACCCTAAGTGTAGCTAAGTTCTCTAGCTACACTTAGGGTCAAGAAAAAAGA

GCT

8. Order oligos from IDT with 5' Phosphate and PAGE purification

3.5.2. Oligo Phosphorylation and Annealing

Phosphorylation of the oligos:

100µM primer1-5 or1-3	0.5µl
T4 PNK (New England biolabs)	1.5µl
T4 PNK buffer (10x)	2µl
H2O	16µl
Final volume	20µl

This mixture was incubated in a water bath at 37˚C for 90 minutes to let phosphorylation occur. The sense and anti-sense oligonucleotides were mixed and heated to 95˚C for 5 minutes, then at 70˚C for 10 minutes followed by gradual cooling to RT.

3.5.3. pLL3.7 vector digestion and dephosphorylation

2 µg of the pLL3.7 vector (Fig.08) was digested using Hpa1 and Xho1 for 1 hour at 37 °C and dephosphorylated using CIP for another 30 mins. The vector was further gel purified and eluted in 20µl of H2O.

Digestion and dephosphorylation of the vector:

2µg vector PlentiLox3.7	1-2µl
Buffer4	2µl
Xho1enzyme	0,5µl
Hpa1 enzyme	0,5µl
H2O	15,8µl
Final volume	20µl

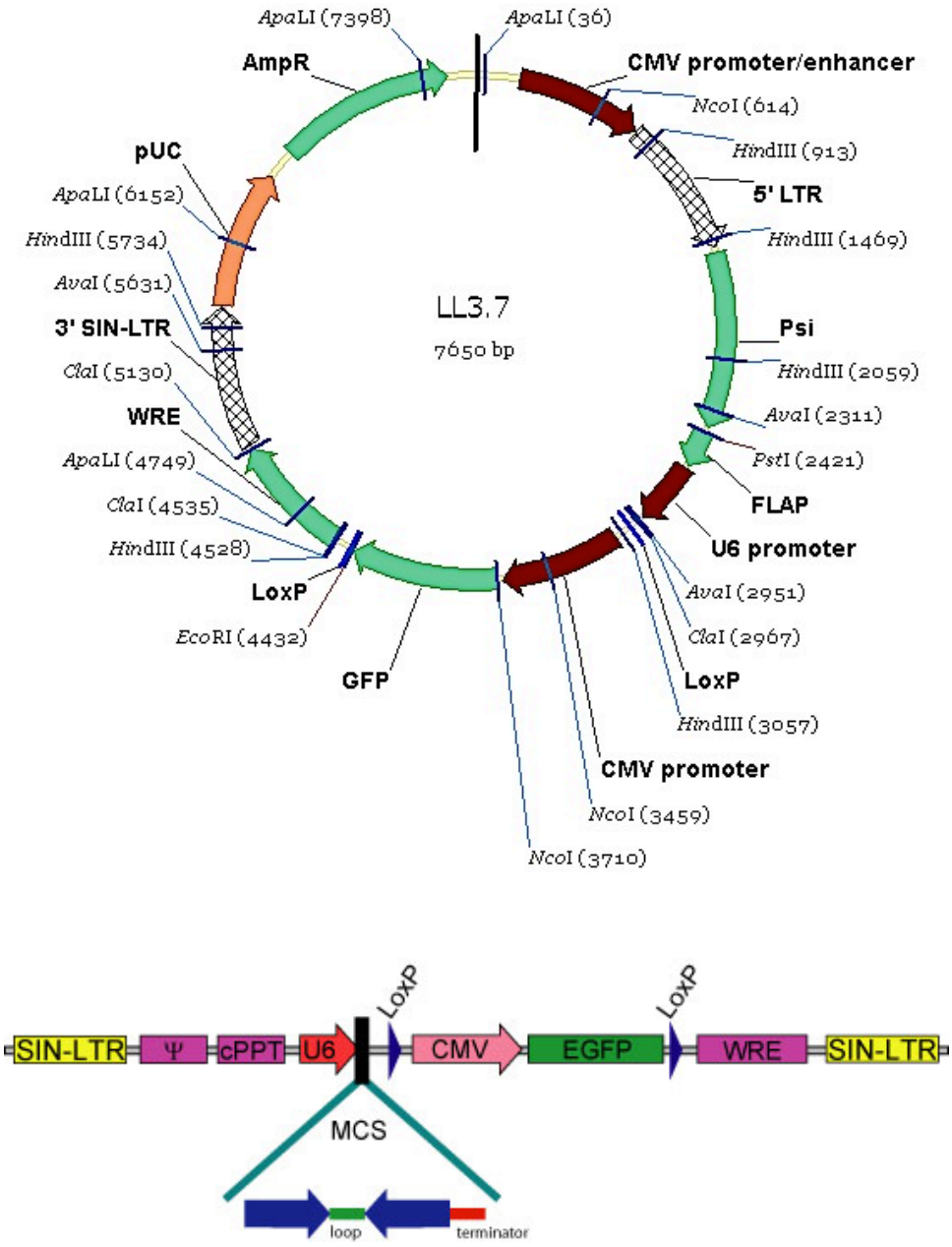

Fig.08: Map of PlentiLox3.7 vector. Showing the MCS (multiple cloning site) and the loop where the construct is inserted into the PlentiLox3.7 vector (Rubinson DA et al, Nature genetics 2003).

3.5.4. Ligation

The phosphorylated oligos and the dephosphorylated vector were then ligated using T4 ligase at 4˚C overnight. DNA ligation is a method to form recombinant DNA constructs by insertion of a restricted fragment into a restricted plasmid vector catalyzed by T4 DNA ligase.

Ligation reaction setup:

Dephosphorylated vector PLLox3.7	2 µl
oligos	1 µl
T4 ligase buffer (10X)	1 µl
T4 ligase	1 µl
Add H2O to	10 µl

3.5.5. Transformation of bacteria

In this thesis we used the heat-shock method to transform recombinant DNA into the bacterial cells. With this method the fast temperature change, in the presence of calcium chloride, leads to a short-term permeability of the competent E. coli for recombinant plasmids. DH5alpha competent E. coli were purchased from Invitrogen. Per transformation experiment, 100µl competent cells were mixed with 5µl ligation product and incubated on ice for 30min. Then the mixture was heat-shocked for 30 seconds at in a 42˚C water bath, immediately followed by incubation on ice for 2 minutes. Subsequently, the competent cells were further cultured in 1ml SOC-medium and shaken for 1 hour at 37˚C, then 200 µl of the bacterial culture was plated on $10cm^2$ Agar plates containing 50µg/ml ampicillin and incubated at 37˚C over night. To prepare agar plates, we used hard Agar and heated it in the microwave at power 20 until all became fluid. 0.5ml ampicillin stock solution (50mg/ml) was added to 500ml Agar and then poured onto $10cm^2$ plates. To dispose of any bubbles that might have formed on the surface of the Agar, a Bunsen burner flame was briefly passed over the Agar surface. Colonies on the Agar plates were picked and grown further in 1.5 ml LB medium at 37 °C overnight. DNA was extracted following standard protocol for mini-scale from QIAGEN.

3.5.6. Confirmation

To confirm that the plasmids extracted above contained our targeting sequence of interest (shRNA), they were subjected to digestion with restriction enzymes Not1 and Xba1 at 37˚C. Similar digestion reaction was also set up for pLL3.7 empty vector. Specifically, the digestion reactions were set up as following.

Digestion reaction setup:

Empty vector PLLox3.7 or plasmids extracted (1ug/ul)	5 µl
BSA(10X)	2 µl
Buffer 3	2 µl
Not1	1 µl
Xba1	1 µl
Add H2O to	20 µl

A 2% agarose gel was run at 150V constantly confirming the ligation product.
After obtaining positive colonies, the plasmids containing the targeting sequence of interest were amplified in a midi-scale following standard protocol from QIAGEN.

3.6. HEK293T cell transfection and NTera2 cell infection

Having successfully cloned and amplified the constructs with our targeting sequence of interest (pLL3.7 control or PTDSR shRNA), these constructs were then transfected into HEK293T cells together with other packaging vectors necessary to produce viruses for infecting NTera2 cells, including pMDLg/pRRE, CMV-VSVG and RSV-Rev (Barde I et al, 2010). Specifically, HEK293T cells were maintained in Dulbecco's Modified Eagle Medium (MEM) (1X), liquid (low glucose), with 10% fetal bovine serum (GIBCO, cat# 10567). The ratios of the plasmids being transfected were as follows.

Packaging mix for a 4 plasmid system:	pLL3.7 : 5µg
	PMDL : 5µg
	VSVL : 3µg
	REV : 2µg

For each $10cm^2$ plate, a total of 15µg DNA was transfected using Lipofectamin 2000 (INVITROGEN). 48 hours post transfection, supernatant containing the lentiviral

particles was filtered through 4.2µm microfilters, collected and span down through ultra-speed centrifugation. The concentrated viruses were then resuspended in cold PBS and kept at -80 freezer for future usage. To infect NTera2 cells, viruses collected from one $10cm^2$ plate were divided into 3 wells of a 6-well plate, which were then treated with RA for different lengths of time before RNA extraction.

3.7. Cloning Flag-PTDSR expression vectors

To determine whether PTDSR binds to certain genomic regions, such as the Hox gene promoter regions, a stable cell line was established expressing Flag-tagged PTDSR. The CMV10 backbone (SIGMA-ALDRICH), includes the binding site for several highly specific ANTI-FLAG monoclonal antibodies (M1, M2, M5) and polyclonal antibodies and conjugates, each with different recognition and binding characteristics, so it can be distinctively detected (Fig.12). PTDSR cDNA sequences were amplified by standard PCR using KOD Hot start DNA polymerase (Novagen).

Component	Volume	Final Concentration
10X Buffer for KOD Hot Start DNA Polymerase	5 µl	1X
25 mM $MgSO_4$[a]	3 µl	1.5 mM
dNTPs (2 mM each)	5 µl	0.2 mM (each)
PCR Grade Water	X µl	
Sense (5') Primer (10 µM)	1.5 µl	0.3 µM
Anti-Sense (3') Primer (10 µM)	1.5 µl	0.3 µM
Template DNA[b]	Y µl	
KOD Hot Start DNA Polymerase (1 U/µl)	1 µl	0.02U/µl
Total reaction volume	**50 µl**	

Tab.14: Standard reaction set up for PCR using KOD Hot start DNA polymerase by Novagene.

Step	Target size			
	< 500 bp	500–1000 bp	1000–3000 bp	> 3000 bp
1. Polymerase activation	95°C for 2 min	95°C for 2 min	95°C for 2 min	95°C for 2 min
2. Denature	95°C for 20 s	95°C for 20 s	95°C for 20 s	95°C for 20 s
3. Annealing	Lowest Primer Tm°C for 10 s			
4. Extension	70°C for 10 s/kb	70°C for 15 s/kb	70°C for 20 s/kb	70°C for 25 s/kb
Repeat steps 2–4	20–40 cycles. For more information see "Cycle number" below			

Tab.15: PCR cycling conditions (NOVAGENE). The PTDSR cDNA is 1.2kb in length, so the extension time specified for this target size was chosen (i.e. 70°C for 20s/kb).

3.8. Western blot

Cells were washed with PBS, scraped and collected by centrifugation. The cell pellets were then lysed with lysis buffer (50 mM Tris HCl, pH 7.4, with 150 mM NaCl, 1 mM EDTA, and 1% TRITON X-100) on ice for 30 minutes. Insoluble fractions and cell debris were removed through centrifugation at 14000 rpm at 4 ^{o}C for 15 minutes. The resultant supernatant was subjected to protein concentration measurement using Bradford assay (Bio-Rad). After determining the protein concentration, precast gels from Invitrogen (NuPAGE Novex 4-12% Bis-Tris gel) were used to separate the protein samples. Briefly, around 30µg of protein samples were loaded for each well. To estimate the target protein size, SeeBlue Plus2 Pre-Stained standard protein marker was also loaded. The gels were run at a constant 150v. To directly visualize the protein bands, Coomassie brilliant stain solution (Invitrogen Inc.) was used. Briefly, protein gel was washed with H_2O for 5 minutes before staining for 1 hour at RT. To detect the proteins by immunoblotting, transfer was performed using the nitrocellulose membrane (Biorad) following the standard procedure. After transfer, the membranes were blocked for one hour at RT using 5% milk/TBST buffer (50 mM Tris.HCl, pH 7.4, 150 mM NaCl, 0.1% Tween 20) followed by adding primary antibody (1:1000 in 5% milk/TBST) for another hour at RT. The membrane was then washed 5 times in TBST before adding the corresponding HRP- conjugated secondary antibody (1:5000 in 5% milk/TBST) for one hour at RT. The membranes were then washed extensively with TBST before chemiluminescent detection. The blot was incubated for one minute in a mixture containing detection solutions 1 and 2 (Amersham, USA) in the ratio 1:1 before exposure and developing.

4. Results

4.1. ChIP-qPCR data

After performing ChIP on the NTera2 cells as described in section 3.4, quantitative PCR (qPCR) was used to determine how much DNA of interest had been precipitated by ChIP using antibodies specific for Flag-PTDSR. The qPCR instrument allows quantitative detection of PCR products as they accumulate during PCR cycles (26-30 cycles). In the amplification curve (left panel, Fig.09), fewer cycles are needed to reach certain amount of products, meaning that more DNA has been precipitated for this particular sample and vice versa. The right panel in Figure 09 shows a dissociation curve with a single peak for a primer set designed for one of the Hox genes tested (HoxA1), suggesting the specific amplication of the target DNA fragment. Similarly, specific primers were designed for all the Hox genes tested.

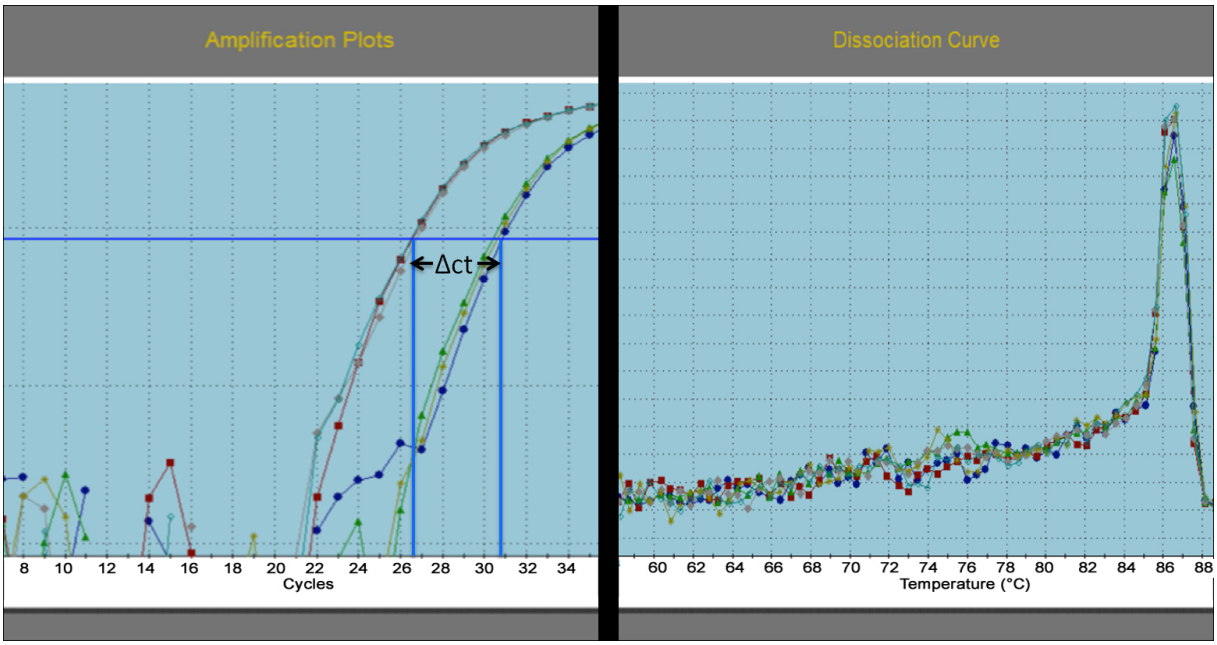

Fig.09: Example of qPCR amplification plot and dissociation curve: X- and Y-axes represent cycle number and fluorescence intensity, respectively**. Left panel:** The blue line shows the PCR cycle numbers needed to reach certain amount of PCR amplication products for different samples, which was arbitrarily chosen in the linear range. Δct means differential cycles between different samples. **Right panel:** dissociation curve showing specific amplication of target DNA fragments, which was performed after a completed PCR amplification. Conditions of qPCR set up: NTera2(RA)PTDSRsiRNA(Hox genes)1SYBR Green dye, 20Hr 45Min.mxpro. Procedure of qPCR as described above.

4.2. Cloning PTDSR shRNA lentivirus vector

DNA from mini-preparation was subjected to digestion with restriction enzymes NotI and XbaI at 37˚C. Similar digestion reaction was also set up for pLL3.7 empty vector. If clones had the PTDSR shRNA sequences inserted, a band shift of 60bp should be observed comparing with the control empty pLL3.7 vector after gel electrophoresis. As shown in Fig.10, two colonies for each PTDSR shRNA cloning were selected for mini-preparation and subjected to digestion along with an empty vector (pLL3.7). One positive clone was obtained for PTDSR shRNA1 and two were obtained for each of the other PTDSR shRNA 2, 3 and 4 respectively. Further sequencing confirmed the presence of PTDSR shRNA sequences in all the positive colonies.

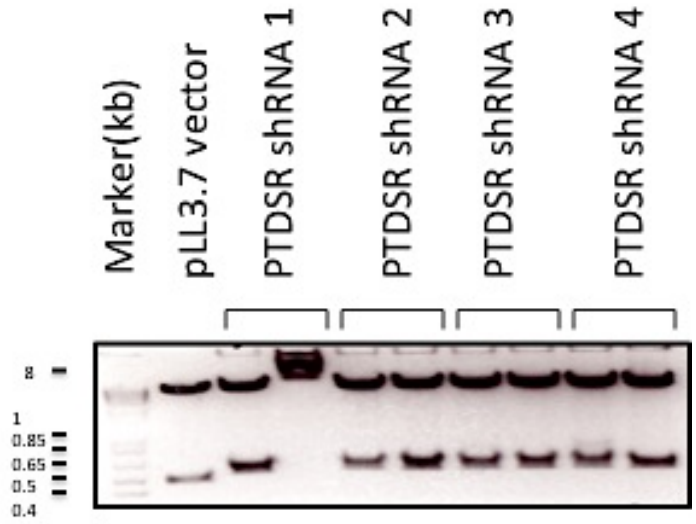

Fig.10: Agarose Gel electrophoresis. DNA was separated by agarose gel electrophoresis (2%) after enzyme digestion. DNA size is shown by DNA marker (lane 1).

4.3. siRNA transfection

To evaluate PTDSR effects on HOX gene expression, a siRNA specific against PTDSR or control siRNA was transfected into NTera2 cells following standard protocols. Lipofectamin 2000 from Invitrogen was used for transfection and the cells were treated with RA 48 hrs after transfection. After 72 hours of RA treatment, mRNA was extracted from the cells and subjected to RT-qPCR to examine the PTDSR siRNA efficiency. As shown in Fig.11, there was no significant change of PTDSR mRNA levels in PTDSR siRNA transfected cells compared with control samples.

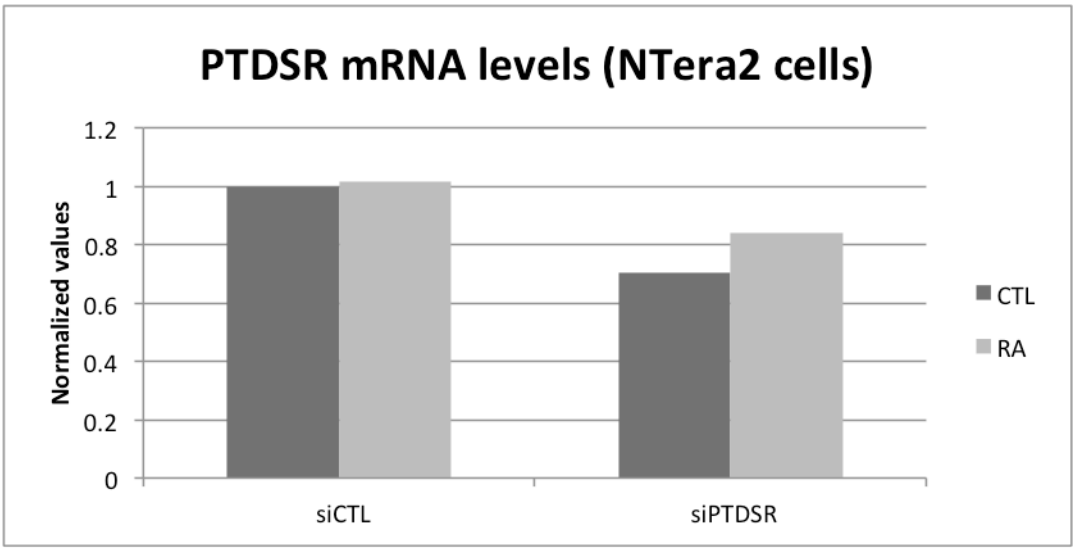

Fig.11: PTDSR mRNA levels examined by RT-qPCR in Ntera2 cells. PTDSR mRNA expression levels in control (CTL) or PTSR siRNA transfected NTera2 cells treated with or without RA for 72 hrs (10-6M). The PTDSR expression was normalized to actin, a house-keeping gene.

4.4. Cloning Flag-PTDSR expression vectors

Because of no sufficient antibodies for detecting endogenous PTDSR proteins in our experiments, the aim was to establish a stable cell line expressing Flag-tagged PTDSR to determine whether it binds to certain genomic regions, such as Hox gene promoters. To achieve the FLAG-tagged PTDSR expression vector, PTDSR cDNA sequences were amplified by standard PCR using KOD Hot start DNA polymerase (Novagen) and cloned into p3xFLAG-CMV-10 expression vector. The entire region of coding sequence was sequenced by DNA sequencing. Not1 and BamH1 were the restriction enzymes used for cloning.

The CMV10 backbone (SIGMA-ALDRICH) includes the binding site for several highly specific ANTI-FLAG monoclonal antibodies (M1, M2, M5) and polyclonal antibodies and conjugates, each with different recognition and binding characteristics, so it can be distinctively detected (Fig.12).

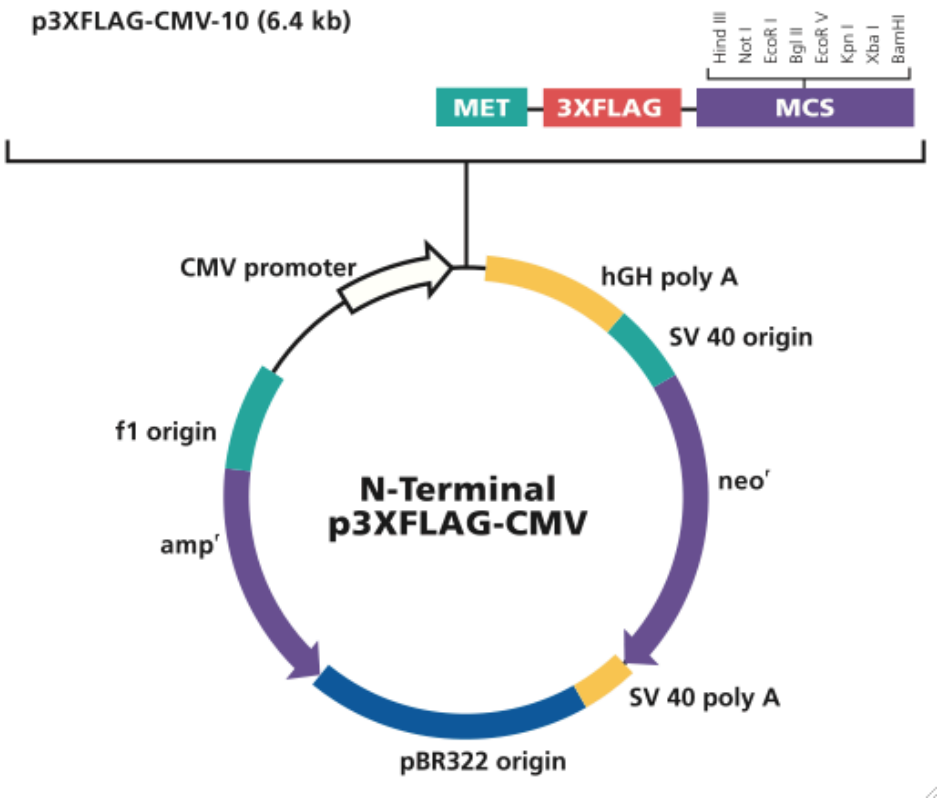

Fig.12: Cloning and expression vector 3XFLAG-CMV-10. Vector map and multiple cloning site (SIGMA-ALDRICH)

4.5. PTDSR shRNA efficiency measured by immunoblotting

As described above, the positive colonies carrying the correct inserts were selected for maxi-preparation, subjecting them to the restriction enzymes Not1 and BamH1, followed by gel electrophoresis. The positive constructs were then transfected into HEK293T cells along with the packaging vectors, VSVG, PMDL and REV. Viruses were collected and used for NTera2 cell infection following standard protocols. The total cell lysates were subjected to immunoblotting analysis with monoclonal M1 antibodies specific for Flag-tagged PTDSR. As shown in Fig.13, all four shRNA sequences, aiming to knock-down PTDSR, worked to different degrees. PTDSR shRNA 2 had the highest knock-down efficiency as indicated in the immunoblot. PTDSR shRNA 1 and 4 expressed higher PTDSR protein levels, indicating that those shRNAs did not knock-down PTDSR well enough. Actin was used as a loading control to demonstrate that equal amounts of proteins were loaded for each sample.

Taken together, PTDSR shRNA2 was chosen for further infecting NTera2 cells to test the PTDSR regulation on its potential target genes.

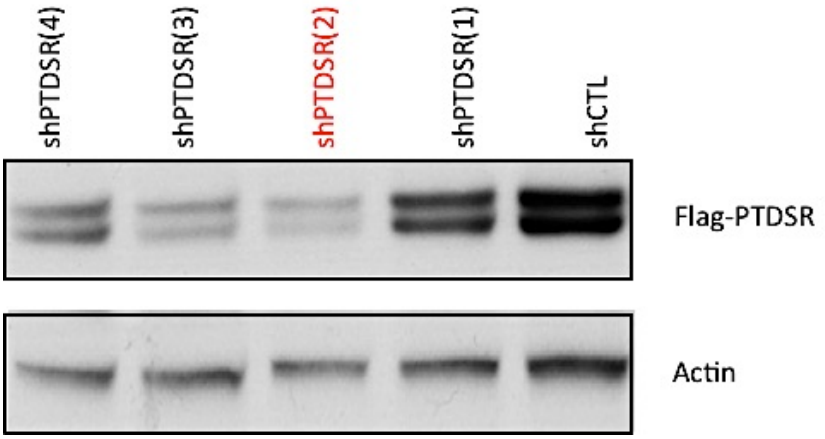

Fig.13: PTDSR protein levels detected by immunoblotting. NTera2 cells were infected with PTDSRshRNA lentiviruses and then total cell lysates were prepared and subjected to immunoblotting using antibody as indicated. Actin was used as control.

4.6. Hox and neural gene transcriptional regulation by PTDSR

NTera2 cells infected with PTDSR shRNA 2 lentivirus were treated with or without RA for 24, 48 and 72 hours. mRNA was then extracted to examine the PTDSR expression levels. As shown in Fig.14, the PTDSR shRNA led to a significant decrease of PTDSR mRNA levels compared to control samples at any given time point.

Since many of late Hox genes and neural genes are activated only after long-term RA treatment, only samples treated with RA for 3 days (72 hrs) along with the controls were submitted to UCSD biogem core facility for microarray analysis.

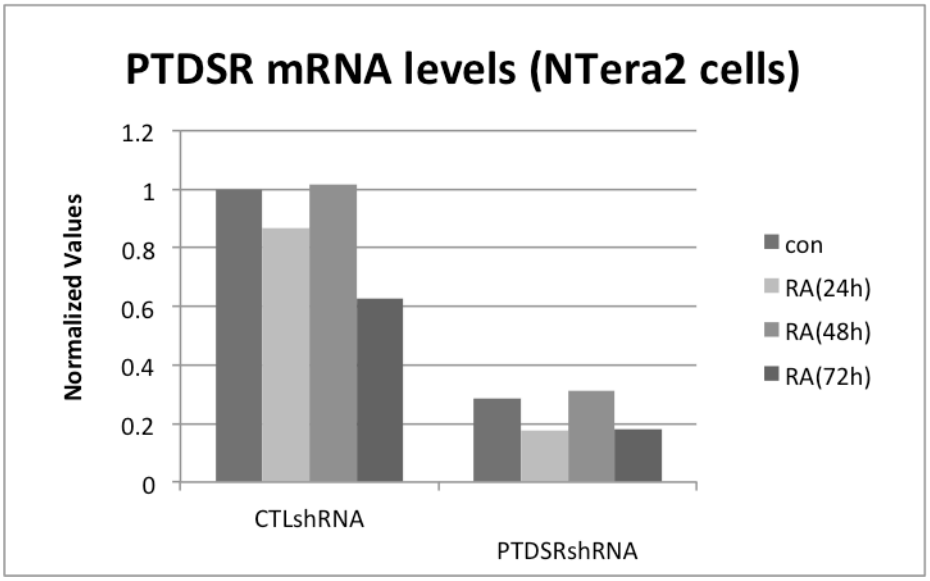

Fig.14: RT-qPCR analysis of the PTDSR mRNA levels in NTera2 cells. PTDSR mRNA expression levels in control or PTSR shRNA infected NTera2 cells treated with or without RA for different time points as indicated (10-6M). The PTDSR expression was normalized to actin, a house-keeping gene.

4.7. Microarray analysis

To achieve an mRNA or gene expression profile we have performed microarray analysis. Here the expression levels of thousands of genes are simultaneously monitored to study the further effects of RA treatment or PTDSR on gene expression.

As shown in Fig.15, there were 558 and 541 genes upregulated or downregulated by RA treatment for 3 days (72 hrs) in NTera2 cells, respectively. Interestingly, among those 558 genes being upregulated by RA, induction of 171 genes by RA was significantly impaired when cells were infected with PTDSR shRNA lentiviruses, suggesting PTDSR might function as a coactivator. In contrast, there were only 14 genes which were further activated in the absence of PTDSR, indicating a repressive function of this enzyme. The rest of the genes (373) showed a PTDSR-independent expression under RA treatment.

Gene ontology analysis revealed regulation of cell size and growth, regulation of transcription, skeletal development, blood vessel development and angiogenesis; protein acid glycosylation and neuron differentiation and neurite morphogenesis were the enriched terms for genes that PTDSR functions as a coactivatior. Specifically, the activation of many of the Hox genes, which encode for transcription factors, as well as some genes involved in neurogenesis, such as DIx5, Pax6, COUP-TF I, COUP-TF II, REST co-repressor 2, contactin2(CNTN2), RHOC and SLIT, were significantly affected while knocking down PTDSR.

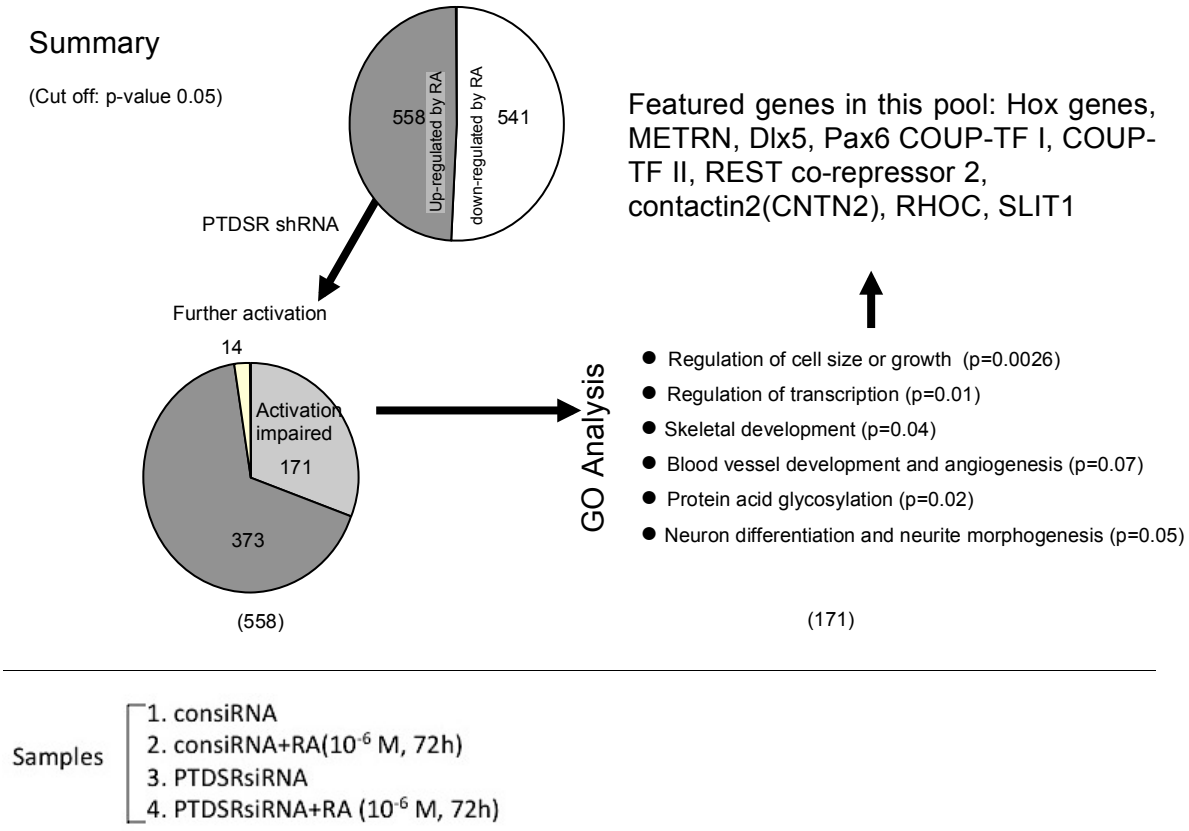

Fig.15: RNA profiling (Microarray analysis) in NTera cells. NTera2 cells infected with PTDSR shRNA 2 lentivirus were treated with or without RA (10-6M) for 72 hours. Total mRNA was then extracted and subjected to RNA profiling. Gene ontology analysis was used to identify biological processes of the tested genes.

4.8. Validation of microarray data through RT-qPCR

4.8.1. Hox gene regulation by PTDSR

Hox genes and those neural genes examined in the microarray analysis were identified to be regulated by PTDSR. As this could potentially contribute to the phenotypes observed for PTDSR knock-out mice, the influence of PTDSR on the expression of these genes was further validated by standard RT-qPCR. There are 39 known HOX genes in the human genome, located on the chromosomes 7, 17, 12 and 2, as summarized in Fig.16. Strikingly, nearly all the early responsive Hox genes require PTDSR for full activation, whereas the late ones show a rather variable activation pattern (see 5.2). As reported, many of late-responsive Hox genes were not inducible by RA treatment after 3 days (Coyle DE, 2011). For those indeed getting activated in this experimental set-up of 3-day-treatment with RA, PTDSR could function as either

coactivator or -repressor on gene expression, indicating a certain pattern of PTDSR impact (Fig.16).

Summary: (39 Hox genes)	
Inducible by RA, PTDSR is required for activation:	+
Inducible by RA, PTDSR functions as a repressor:	-
Inducible by RA, PTDSR had no effects:	0
Non-inducible by RA:	N/A

Tab.16: Regulation of Hox genes by PTDSR under RA stimulation. Hox genes were divided into four different catagories based on their activation status by RA and PTDSR.

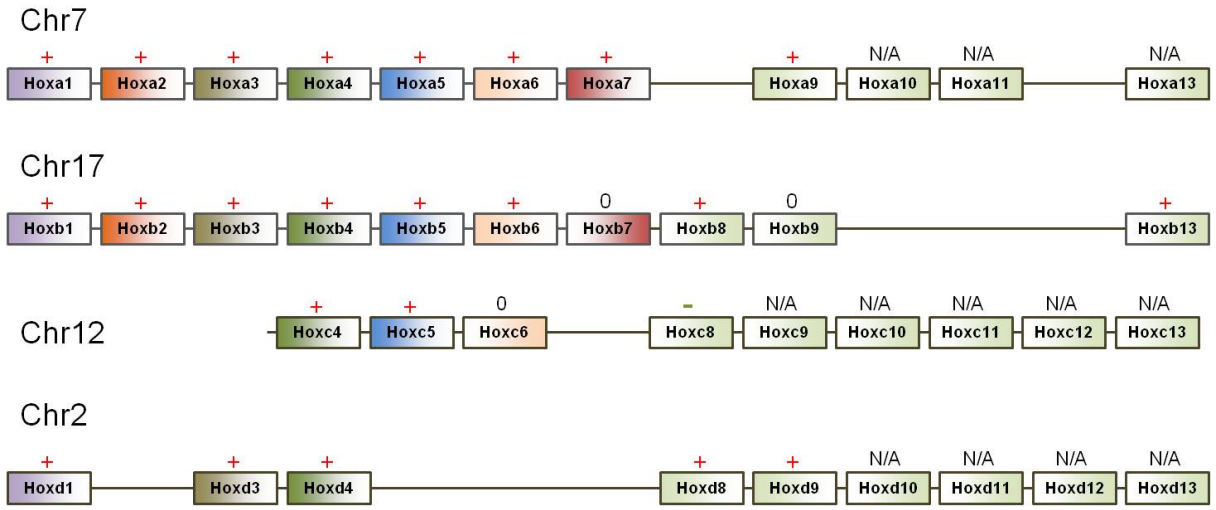

Fig.16: Regulation of Hox genes by PTDSR under RA stimulation. Schematic representation of all four Hox gene clusters in human genome. The chromosomal location of each cluster is indicated on the left. Regulation of RA and PTDSR on these Hox genes is marked as described in Table 16 on top of each individual gene.

4.8.1.1 HoxA cluster regulation by PTDSR examined by RT-qPCR

To test for the PTDSR requirement for RA activation of HoxA genes, the expression levels of all HoxA genes under normal and +RA conditions and under PTDSRsiRNA were examined. After mRNA was extracted, qPCR was performed to quantify relative HoxA mRNA levels in order to determine the effect of PTDSRsiRNA in the -RA and +RA conditions. Most of the early responsive HoxA genes (A1-A7) demonstrated the expected up-regulation by RA treatment, as well as a significant dependence on PTDSR expression for this up-regulation (Fig.17). HoxA6 seemed to show the same behavior, unfortunately not enough replicates worked to determine significance. Most late HoxA genes (A9-A13) did not show to be induced by RA, with HoxA9 being the

exception, whose up-regulation was also PTDSR-dependent. Interestingly, HoxA10 expression seemed to increase in an RA-dependent manner only upon PTDSR depletion, suggesting a negative regulatory effect of PTDSR on this gene. HoxA11 levels were not significantly affected by RA and/or PTDSR depletion. Finally, HoxA13 levels were negatively regulated by RA, which is enhanced by PTDSR depletion.

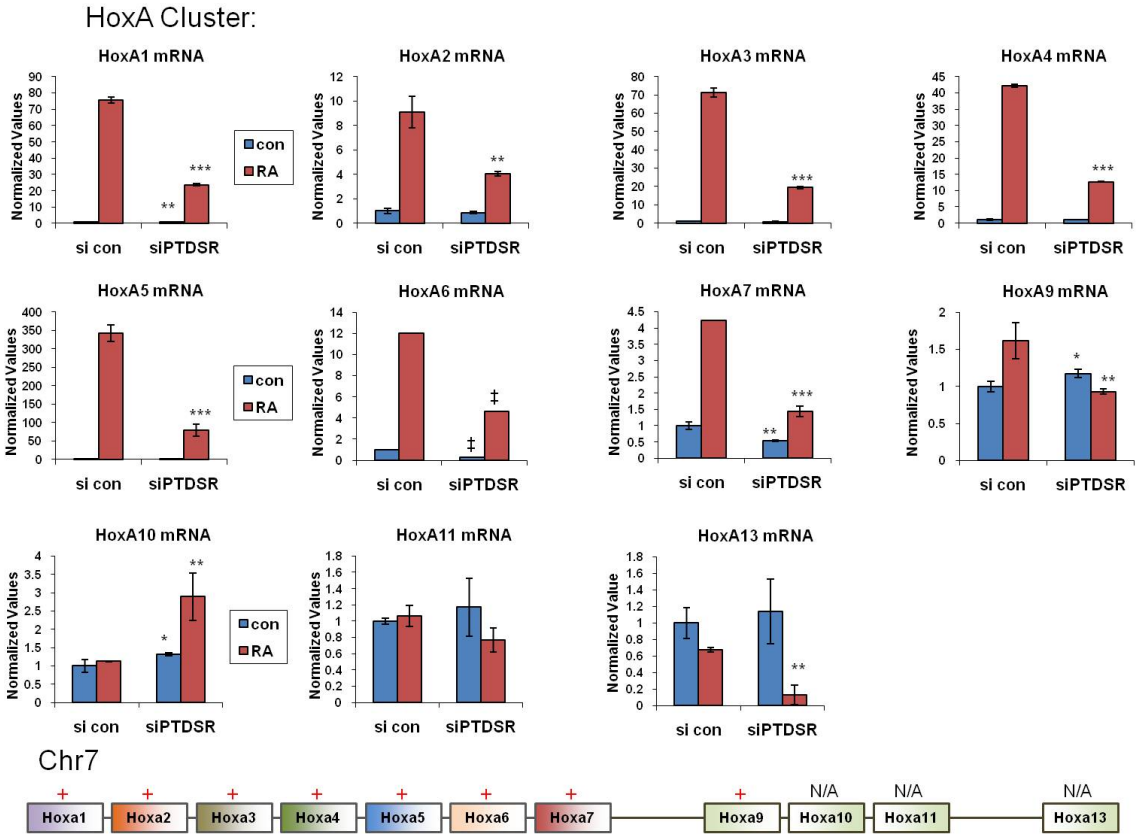

Fig.17: HoxA cluster regulation by PTDSR examined by RT-qPCR. HoxA cluster mRNA expression levels in control or PTDSR siRNA infected NTera2 cells treated with or without RA for 72 hrs (10-6M). The expression of each individual gene was normalized to actin, a house-keeping gene (p-value: *P <0.05, **P <0.01, ***P <0.001).

4.8.1.2 HoxB cluster regulation by PTDSR examined by RT-qPCR

HoxB genes' mRNA levels were similarly quantified and tested under +/-RA and +/-PTDSRsiRNA conditions (Fig.18). Early HoxB genes (B1-B7) generally showed a clear RA up-regulation and all but HoxB7 also had PTDSR-dependence for these enhanced expression levels. Late HoxB genes (B8-B13) also showed a clear RA up-regulation with HoxB8 and HoxB13 demonstrating PTDSR-dependence. However, HoxB9's RA-

induced up-regulation was unaffected by PTDSR depletion, and oddly had a slight but significant PTDSR negative regulatory effect in -RA conditions.

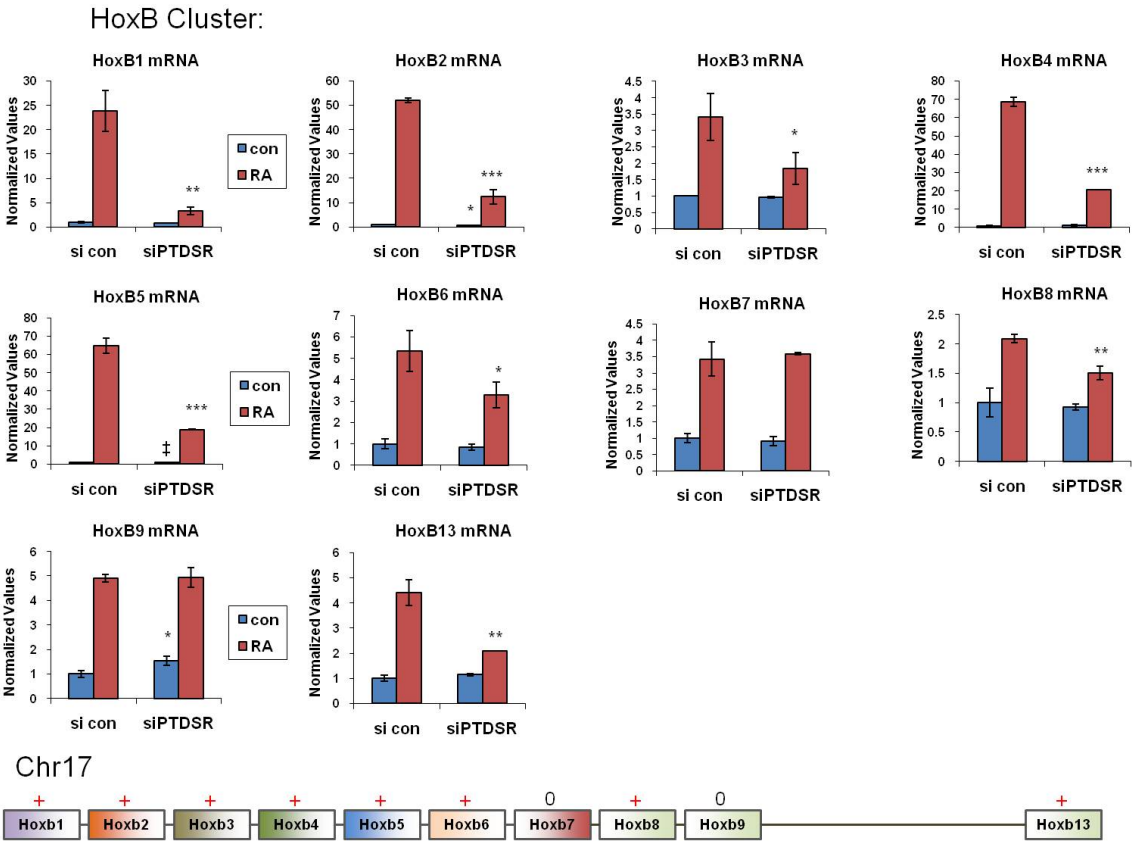

Fig.18: HoxB cluster regulation by PTDSR examined by RT-qPCR. HoxB cluster mRNA expression levels in control or PTDSR siRNA infected NTera2 cells treated with or without RA for 72 hrs (10-6M). The expression of each individual gene was normalized to actin, a house-keeping gene (p-value: *P <0.05, **P <0.01, ***P <0.001).

4.8.1.3 HoxC cluster regulation by PTDSR examined by RT-qPCR

HoxC genes were interrogated for RA-inducibility and PTDSR dependence as described earlier. Early HoxC genes (C4-C6) did not show a clear trend for regulation (Fig.19). HoxC4 was RA-inducible and markedly PTDSR-dependent. HoxC4's basal expression was also PTDSR-dependent. HoxC5 showed no RA-dependent expression changes, however the basal expression levels were negatively affected by PTDSR knockdown. HoxC6 showed no clear regulation by RA or PTDSR. Late HoxC genes (C8-C13) also had a myriad of regulatory patterns, though generally they were RA-irresponsive. HoxC8 was not RA inducible, however it was under significant repression

by PTDSR, as evidenced by the up-regulation of this gene's mRNA levels upon siPTDSR treatment. HoxC10 seemed to be only under PTDSR control under basal conditions where it showed decreased expression levels under PTDSR knockdown. HoxC11 also had no basal RA-dependence, however under PTDSRsiRNA conditions the basal expression level drops only under +RA treatment. HoxC12 seemed to require PTDSR for maintaining basal expression levels, irrespective of RA treatment. HoxC13 showed a clear RA-dependent down-regulation, however this regulation is lost when PTDSR is knocked down. Interestingly, PTDSR seems to play a positive role in basal expression of HoxC13, but then loses its regulatory capacity in +RA conditions. It should be noted that HoxC9 seems to show a pattern similar to that of HoxC13, though not enough replicates were successfully evaluated to determine significance.

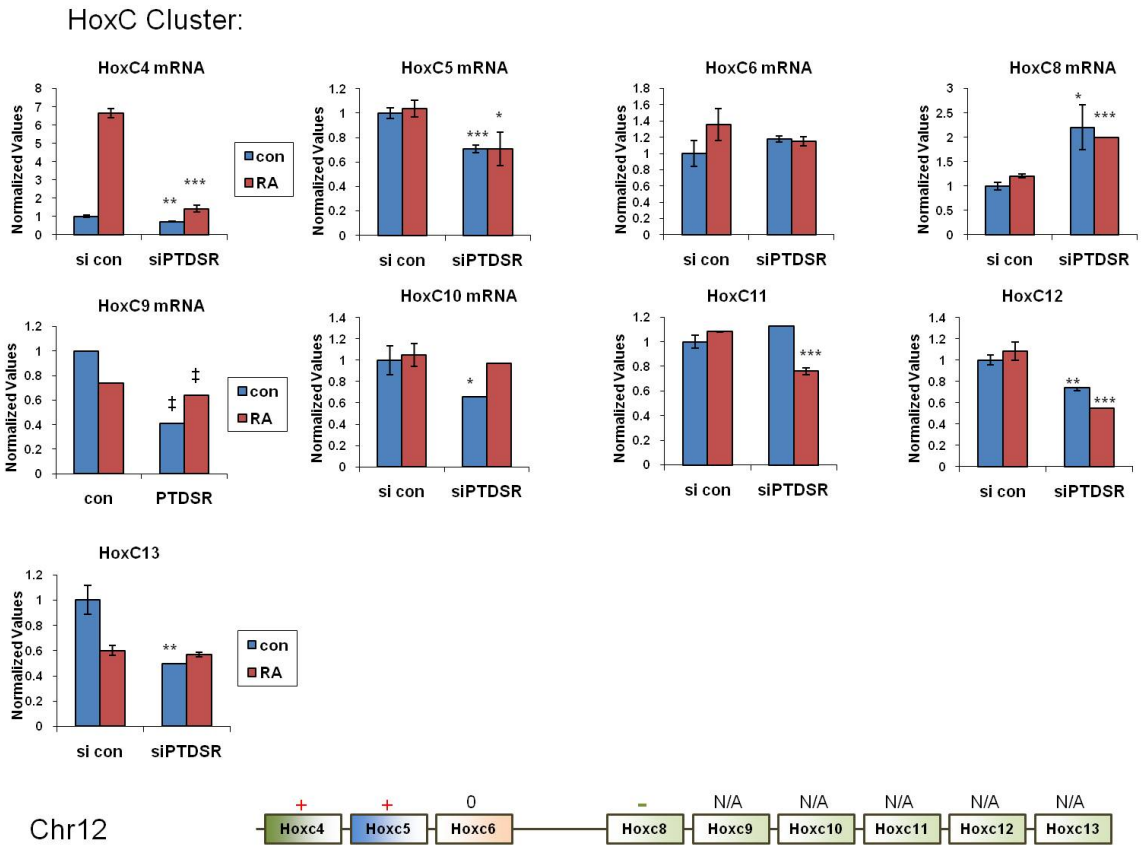

Fig.19: HoxC cluster regulation by PTDSR examined by RT-qPCR. HoxC cluster mRNA expression levels in control or PTDSR siRNA infected NTera2 cells treated with or without RA for 72 hrs (10-6M). The expression of each individual gene was normalized to actin, a house-keeping gene (p-value: *P <0.05, **P <0.01, ***P <0.001).

4.8.1.4 HoxD cluster regulation by PTDSR examined by RT-qPCR

Gene expression levels of HoxD genes were assayed as before. Early HoxD genes (D1-D4) showed a RA-dependent up-regulation as displayed in Fig.20. Of the three early HoxD genes, HoxD1 and HoxD3 showed that PTDSR was involved in this up-regulation by RA. HoxD4 displays a similar trend, though not enough replicates could be evaluated to show significance. Late HoxD genes (D10-D13) generally had a negative response to RA treatment, and in all cases they had a PTDSR-dependent regulatory effect. HoxD10 levels seemed to be repressed by PTDSR in both - and + RA conditions. In HoxD11 levels, though unaffected by PTDSR in -RA, the down-regulation by RA could be rescued by PTDSR knock-down. HoxD12 seemed to require PTDSR to maintain expression levels in both the basal and +RA conditions, as did HoxD13.

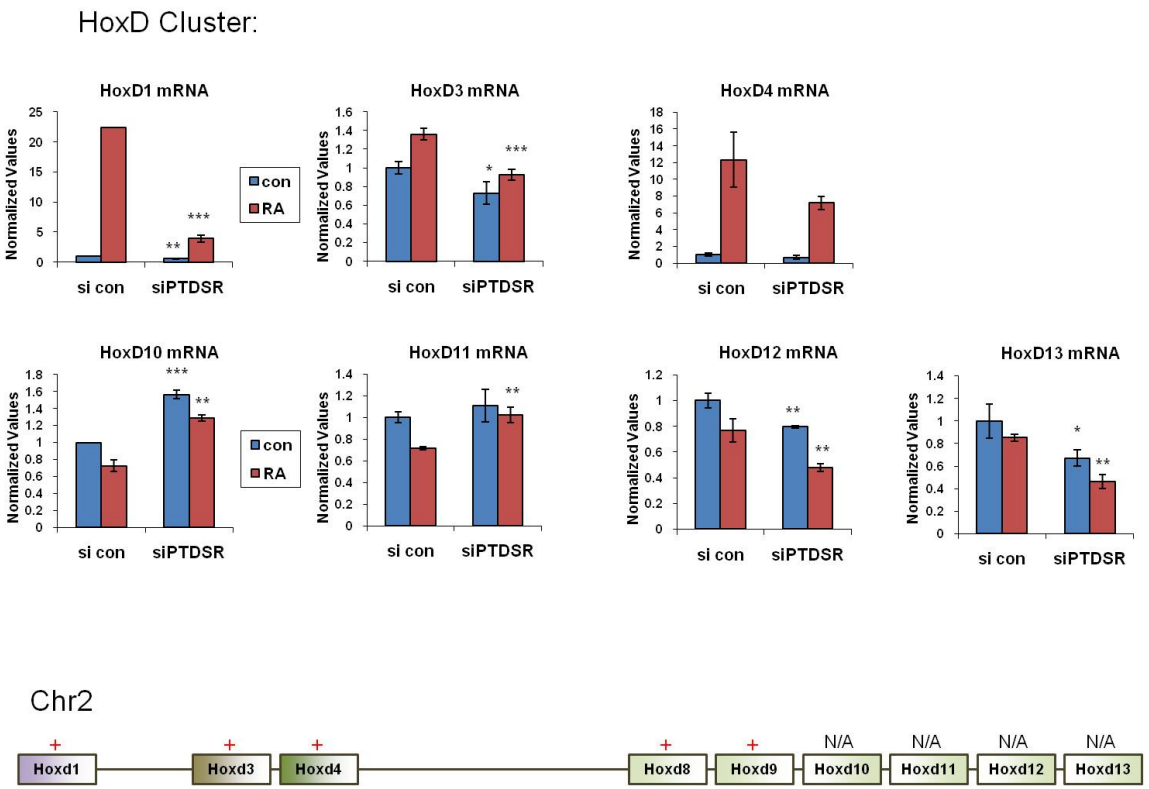

Fig.20: HoxD cluster regulation by PTDSR examined by RT-qPCR. HoxD cluster mRNA expression levels in control or PTDSR siRNA infected NTera2 cells treated with or without RA for 72 hrs (10-6M). The expression of each individual gene was normalized to actin, a house-keeping gene (p-value: *P <0.05, **P <0.01, ***P <0.001).

4.8.2. Neural genes regulation by PTDSR

The NTera2 cell line, which is derived from human teratocarcinoma, exhibits similar properties as embryonic stem (ES) cells or very early neuroepithelial progenitors. NTera2 cells can be induced with RA to become postmitotic central nervous system neurons. They are widely used as a model system for differentiation of cells from the neural lineage (Briscoe J et al, 2000). Therefore, we concentrated our efforts on validating the effects PTDSR had on the expression of these genes detected by RNA profiling, such as Pax6, Dlx5, CoREST2, CoupTF I, CoupTF II, Contactin2 and METRN.

Dlx5, a homeobox protein, is also an important regulator for embryogenesis and has been shown to be crucial for osteogenic induction during frontal bone development (Chung IH et al, 2010). Another neuronal gene, Pax6, is essential for neural development in the retina (Li T et al, 2006) and its expression has been shown to be inducible by RA in NTera2 cells (Gajovic S et al, 1997). Upstream promoter-transcription factors (COUP-TF I and II) (Fernandez-Rachubinski F et al, 2001) as well as silencing transcription factor Co-REST and others CNTN2 (a member of the immunoglobulin superfamily), RHOC (a small signaling G-Protein) and SLIT1 (secreted glycoprotein activating receptors of the Robo (Hohenester E, 2008) all play an important role in the establishment of neuronal identity (Belyaey ND et al, 2004).

Expression levels of selected neural genes were assayed under -/+RA and -/+ PTDSRsiRNA conditions. All neural genes examined showed a clear up-regulation by RA treatment (Fig.21). Pax6 however showed a major depletion of expression levels under PTDSR control. Dlx5 seemed to show the same pattern, though more replicates are needed to show significance. CoREST2 also showed a drop in expression levels upon PTDSR depletion, though it lost the RA-responsiveness under this condition. CoupTF1 and CoupTF2 showed PTDSR-dependent regulation in the +RA case, while only CoupTF2 also showed this dependence under basal conditions. Contactin2 was under significant positive PTDSR control in both -/+RA conditions. Similarly, METRN was under positive control by PTDSR in both treatment conditions.

PTDSR/ Neurogenesis

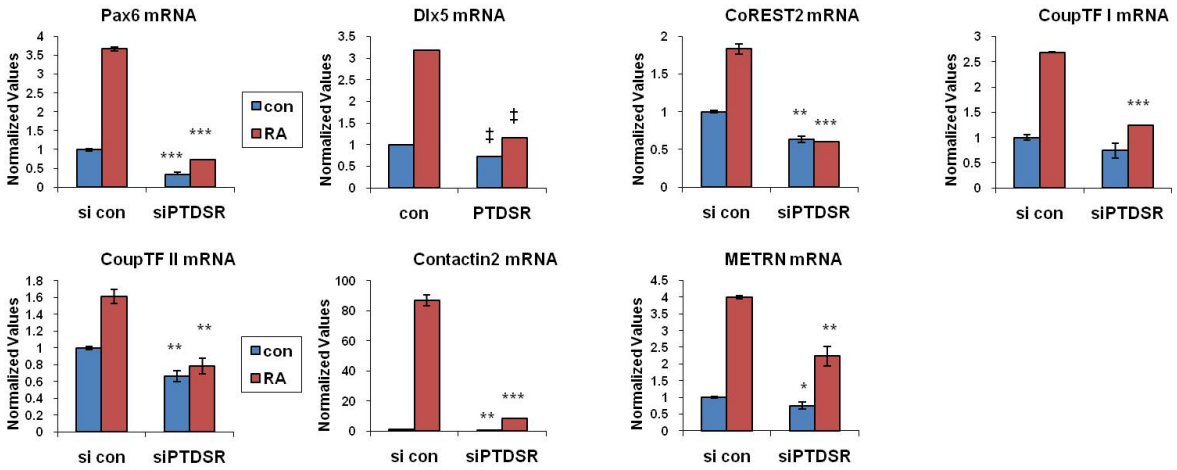

Fig.21: Selected neural genes regulation by PTDSR examined by RT-qPCR. mRNA expression levels of selected neural genes as indicated in control or PTDSR siRNA infected NTera2 cells treated with or without RA for 72 hrs (10-6M). The expression of each individual gene was normalized to actin, a house-keeping gene (p-value: *P <0.05, **P <0.01, ***P <0.001).

4.9. pCMV10-flag-PTDSR cloning

An extensive range of commercially available PTDSR antibodies for ChIP assay was tested, but none of them gave satisfactory results. Therefore, a Flag-tagged PTDSR expression vector was cloned to enable the detection of this protein binding on its potential genomic loci of interest, specifically, Hox genes and neural genes tested above. Flag-tagged PTDSR was cloned following the protocol as mentioned in the section Methods and Materials.

Two colonies were selected for mini-preparation and subjected to digestion with restriction enzymes Not1 and BamH1 at 37˚C. Similar digestion reaction was also set up for the empty vector (pCMV10). If clones contained the Flag-PTDSR sequences inserted, an additional band of around 1.2kb in size would be observed compared with control via gel electrophoresis. Indeed, as shown in Fig.22 panel (a), both selected colonies contained the PTDSR insertion. One of the colonies was further chosen for large scale plasmid purification and transfected into HEK293T cells to check the proper expression of this construct. As shown in Fig.22 panel (b), total cell lysate collected from cells transfected with either control vector (pCMV10) or pCMV10-Flag-tagged PTDSR were subjected to immunoblotting using an antibody specific for Flag epitope.

As expected, a specific band was detected in Flag-tagged PTDSR transfected samples, which corresponded to the right size of this protein. For the loading control, immunoblotting with an antibody specific for GAPDH was also performed in parallel. As shown at the bottom of Fig.22 panel (b), equal amounts of proteins were loaded for the control (pCMV10) and pCMV10-PTDSR.

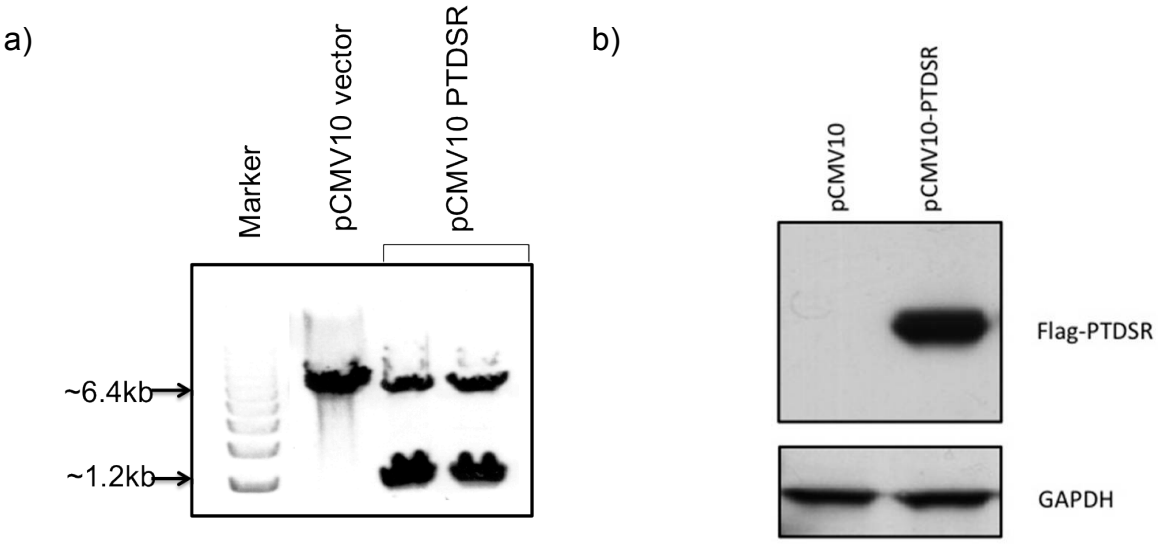

Fig.22: a) DNA Agarose Gel electrophoresis. DNA was separated by agarose gel electrophoresis (1%) after enzyme digestion with Not1 and BamH1. DNA size was shown by DNA marker (1kb DNA ladder) (lane 1). **b) Flag-tagged PTDSR construct validated by immunoblotting**. HEK293T cells were transfected with either control or Flag-tagged PTDSR and then total cell lysates were prepared and subjected to immunoblotting using Flag antibody. GAPDH was used as a loading control.

4.10. PTDSR binding to the promoter regions of selected Hox and neural genes examined by ChIP

Due to the lack of ChIP quality grade PTDSR antibodies and the difficulty of introducing plasmids into NTera2 cells, HEK293T cells were used as a substitute to check the PTDSR binding on selected Hox loci, which have shown to exert similar expression patterns responsive to RA in both cell lines. To detect Flag-tagged PTDSR binding on selected target genes, HEK293T cells were transfected with either an empty vector (pCMV10) or a Flag-tagged PTDSR construct and then treated with or without RA followed by ChIP-qPCR with primers specific targeting to the promoter regions of selected Hox genes. The promoter regions are very CpG-rich in general, which made the successful primer design impossible for some of the Hox gene promoters of interest. Therefore, only selected ones were shown in Fig.23.

Specifically, we focused on the ones which required PTDSR for their full activation by RA, such as HoxA2, A5, A6, A7, B2, B5, B6, C4, C5 and D3. Since PTDSR might function as a co-activator, its binding would be expected to increase upon RA stimulation if it directly targets these genes for activation. HoxA2, A5, B6 and C5 displayed a highly increased binding of Flag-PTDSR under activation +RA compared to the controls with no RA treatment. This data suggests that PTDSR is required for activation of these genes. Hox A7, B2 and C4 showed a stronger PTDSR binding under +RA conditions, but no significant increase compared to –RA conditions.

HoxA6 and B5 promoters showed a decreased binding of PTDSR upon RA induction, suggesting that the effects of PTDSR on the transcriptional activation of these genes might not be through direct binding to their promoters. The binding of PTDSR on HoxD3 promotor was slightly higher after RA induction although no significance was evaluated. The neural genes Dlx5 and Pax6 showed a strong binding of Flag-PTDSR to their promotor region under +RA conditions with a high significance compared to the control (pCMV10) (Fig.23).

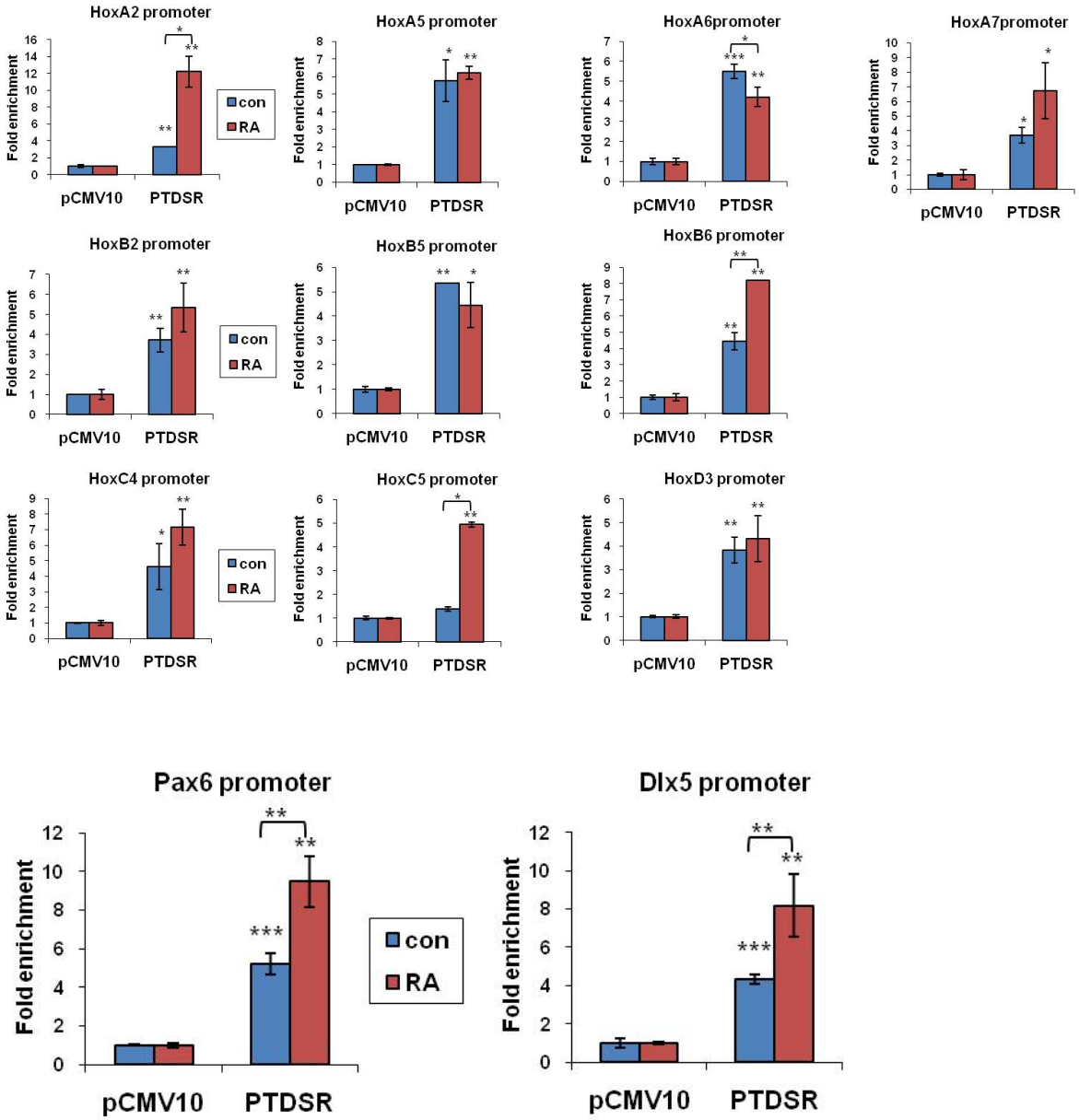

Fig.23: Binding of Flag-PTDSR on selected Hox and neural gene promoter regions detected by ChIP-qPCR. HEK293T cells were transfected with either pCMV10 (empty vector) or Flag-PTDSR and treated with or without RA for 24 hrs (10^{-6}M) followed by ChIP using anti-flag antibody. ChIP signals shown were normalized to that of pCMV10 (p-value: *P <0.05, **P <0.01, ***P <0.001).

4.11. H1K26me3 occupancy on the promoter regions of selected Hox and neural genes examined by ChIP

4.11.1. H1K26me3 occupancy on selected Hox genes

To understand the underlying mechanism of how PTDSR regulates the expression of the Hox and neural genes, I focused on the histone mark H1K26me3. Previous data from the Rosenfeld laboratory showed a specific demethylase activity on this mark. This methylation marker has been shown to be associated with transcriptional repression through binding with HP1 and L3MBTL1 (West LE et al, 2010; Trojer P et al, 2009). Therefore, the occupancy of H1K26me3 on Hox genes was tested after PTDSR knock-down, aiming to see whether it could also demethylate this marker *in vivo* (Fig.24). NTera2 cells were transfected with either control or siRNA against PTDSR followed by ChIP with antibodies specific for H1K26me3. If PTDSR functions as a H1K26me3 demethylase *in vivo*, one would expect that its occupancy increases in the absence of PTDSR on specific loci. Indeed, those selected Hox genes Hox A2, B2, B5, C5 and D3 exhibited a significantly increased occupancy of H1K26me3. Comparing siCTRL and siPTDSR of those genes, a clear rise in the methylation level under PTDSR knock-down is depicted. HoxC4 also showed a strong increase of methylation at its promoter site under siPTDSR conditions. Interestingly HoxB6 showed no significant changes in occupancy of H1K26me3, suggesting additional mechanisms other than PTDSR functioning as a H1K26me3 demethylase must account for this observation.

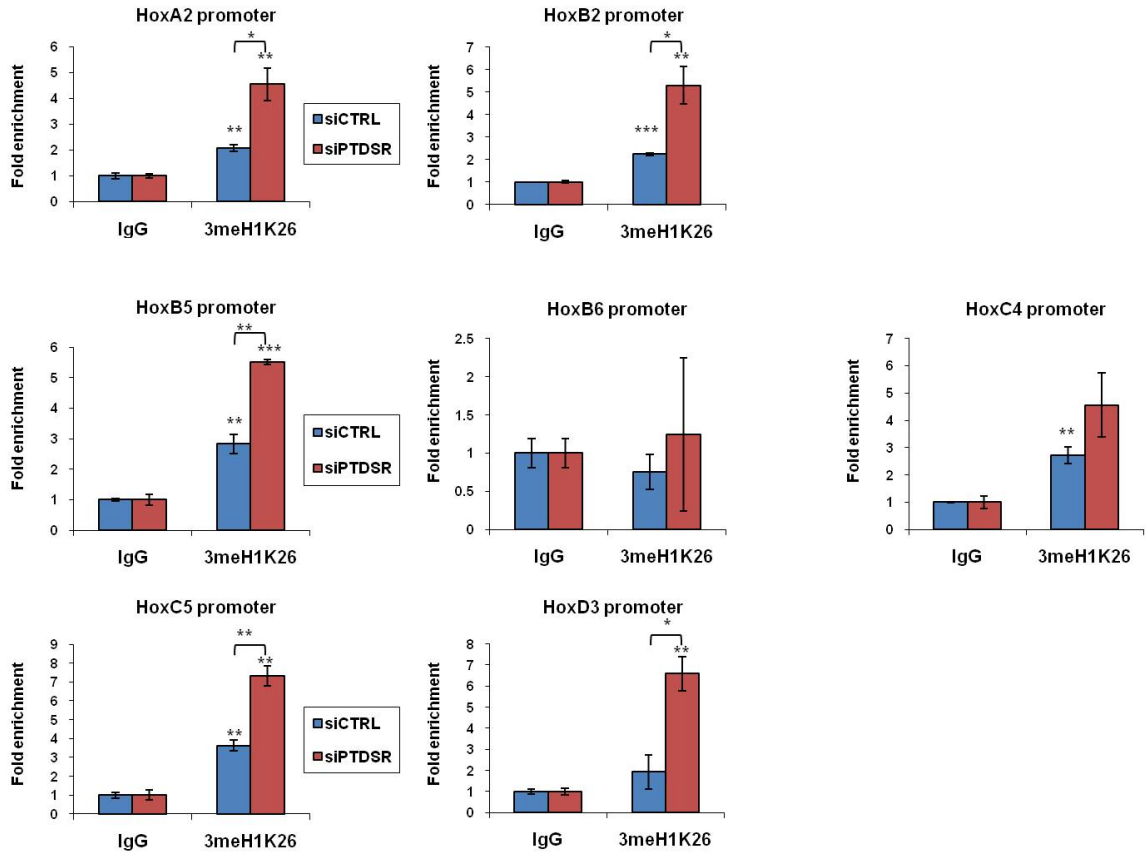

Fig.24: Occupancy of H1K26me3 on selected Hox gene promoter regions detected by ChIP-qPCR. NTera2 cells were transfected with either control or siRNA against PTDSR followed by ChIP using anti-H1K26me3 antibody. The ChIP signals shown were normalized to that of IgG
(p-value: *P <0.05, **P <0.01, ***P <0.001).

4.11.2. H1K26me3 occupancy on selected neural genes

NTera2 cells were transfected as mentioned in 4.11.1. Those selected neural genes, which were shown to require PTDSR for their full activation by RA, were identified through microarray and validated by RT-qPCR. METRN, CoREST2 and Pax6 exhibited a significantly increased occupancy of H1K26me3 in the absence of PTDSR, suggesting it might function as an H1K26me3 demethylase on these specific loci to regulate their expression (Fig.25). Coup TF II as well as Dlx5 promoter region also showed an increased occupancy of H1K26me3 under PTDSR siRNA conditions, though not enough replicates were successfully evaluated to determine significance. No change of H1K26me3 occupancy in the absence of PTDSR suggested additional mechanisms other than functioning as an H1K26me3 demethylase must account for this observation.

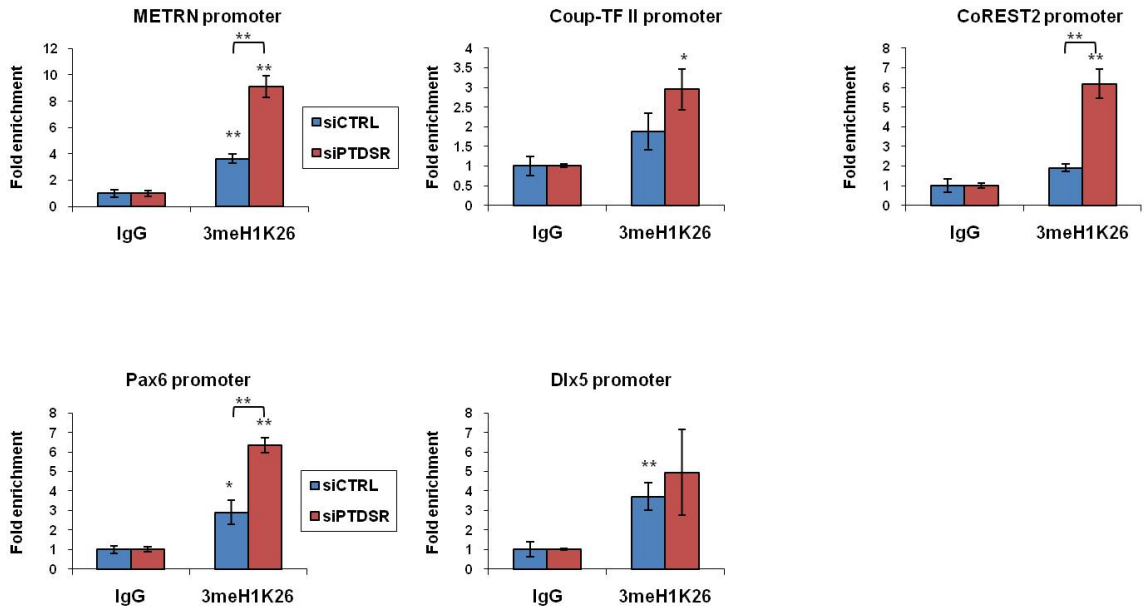

Fig.25: Occupancy of H1K26me3 on selected neural gene promoter regions detected by ChIP-qPCR. NTera2 cells were transfected with either control or siRNA against PTDSR followed by ChIP using anti-H1K26me3 antibody. ChIP signals shown were normalized to that of IgG (p-value: *P <0.05, **P <0.01, ***P <0.001).

5. Discussion

Histone tail methylation is an important part of post translational modifications taking place in the genome. It is an intensely researched topic in the field of molecular biology and has been shown to play a critical role in gene transcription. Recently, the enzymes capable of removing these methylation marks, either on histones or non-histone proteins, were identified. LSD1 was the founding member of demethylases, which directly removes histone H3K4 or H3K9 mono- or dimethyl modifications by an oxidative demethylation reaction in which flavin is a cofactor (Shi Y et al, 2004; Metzger E et al, 2005). In addition, the largest classes of demethylase enzymes, which contain a Jumonji C (JmjC) domain and catalyze lysine demethylation of histones through an oxidative reaction that requires iron Fe (II) and α-ketoglutarate (αKG) as cofactors, have been identified (Tsukada, Y et al, 2006). While LSD1 can only remove mono- and dimethyl modifications, the JmjC-domain-containing histone demethylases (JHDMs) can remove all three histone lysine methylation states. For example, JHDM1 specifically demethylates H3 mono- and dimethylated Lys36 (Tsukada, Y et al, 2006); JHDM2A demethylates H3 mono- and dimethylated Lysine 9 (Yamane K et al, 2006); and JMJD2 family demethylates H3 trimethylated Lysine 9 or Lysine 36 (Whetstine JR et al, 2006; Cloos PA et al, 2006; Fodor BD et al, 2006, Klose RJ et al, 2007) to give rise to dimethylated counterparts. The Jarid1 family demethylates H3 di- and tri-methylated lysine 4 (Christensen J et al, 2007); JMJD3 family demethylates H3 di- and tri-methylated lysine 27 Jepsen, K et al, 2007, Agger K et al, 2007; De Santa F et al, 2007, Lan F et al, 2007); PHF8 family has multiple substrate specificity towards H3 mono- and di- lysine 9 and 27 as well as H4 mono- lysine 20 (Liu W et al, 2010); and JMJD5 demethylates H3 di-methylated lysine 36 (Hsia DA et al, 2010).

The aim of this study was to identify possible biological targets for the JmjC-domain containing enzyme JMJD6/PTDSR. Various steps were taken:

1) Creating a lentiviral vector containing PTDSR shRNA sequence to efficiently knock-down PTDSR in NTera2 cells.

2) Identifying possible biological target genes of PTDSR through mRNA profiling in control and PTDSR shRNA infected NTera2 cells.

3) Illustrating the possible mechanisms by which PTDSR regulates its target genes.

Through biochemical and molecular biology tools, we found that this protein has a broad impact on the Hox family gene expression as well as on some of the critical neural genes involved in neurogenesis induced by RA. The study further tried to address the possible mechanisms by which PTDSR regulates these genes. Specifically, it was demonstrated that PTDSR directly binds to the promoter regions of selected Hox and neural genes. Furthermore, biochemistry data from the Rosenfeld laboratory suggested PTDSR might function as a Histone H1 lysine 26 demethylase to remove this repressive marker. We therefore tested whether this mark increases upon knocking down PTDSR and found that the absence of PTDSR indeed led to increasing levels of H1K26me3, suggesting PTDSR might regulate the expression of the aforementioned genes through demethylating H1K26me3. Nevertheless further studies are needed for understanding the underlying mechanisms of PTDSR regulation. The findings described in this thesis provide possible cornerstones for further investigation of PTDSR by pointing out new aspects in functionality of this protein.

5.1. Role of PTDSR in knock-out mice

As described above, the importance of PTDSR for the correct limb developement has been demonstrated, among others, in the JMJD6-/- knock-out mouse experiments performed by Böse et al (2004). These phenotypes were showing severe anomalies, bringing up the question what biological targets PTDSR regulates in the embryonic differentiation of multiple tissues (Fig.04). PTDSR expression was detected in early developmental stages and remained at a high level in the developing nervous system.

In addition, by knocking out PTDSR in mice, Kunisaki Y et al. (2004) and Ming OL et al. (2003) discovered severe developmental defects in several organ systems which led to early death during the perinatal period. Malformations were especially observed during the fetal lung developement, the retina and in the brain, where altered morphology was noted in the midbrain, brainstem spinal cord junction and cerebellum. Thus, the focus of this study was put on those neural genes and Hox genes identified in microarray experiments performed on NTera2 cells infected with control or PTDSR shRNA lentivirus and treated with or without RA.

5.2. NTera2 cells as a model cell line

Previous studies have shown that, following RA treatment, a proportion of NTera2 cells terminally differentiate to neurons and astroglia (Smith B et al, 2010). Three days (72 hours) after RA treatment, islands of NTera2 cells showed increased expression of neurofilament proteins. By 10-14 days, these cells began to morphologically resemble neurons. Under treatment with RA they follow a highly reproducible neural differentiation program (Pleasure SJ et al, 1993), which made them a model system to use in the experiments of this study. Notably, not all Hox genes were inducible by RA under the applied conditions of treating the NTera2 cells with RA for 72 hours (Fig.16). These results suggest that for the activation of those “later“ genes in the Hox clusters, a longer RA treatment may be needed.

A future experiment would include extending the RA treatment time to 5 days and repeating the RT-qPCR experiments on the currently unaffected Hox genes. If these genes then display RA-inducibility, testing the effect of PTDSR depletion would prove interesting to determine if this protein is required for late Hox gene expression as well. Concomitantly, the expectation for early Hox gene repression at the 5 day RA timepoint would present another interesting aspect of PTDSR function to test whether PTDSR is required for early Hox gene repression, or if PTDSR is removed entirely from this region. ChIP experiments for PTDSR on early Hox promoters could be done at this later timepoint to provide evidence for possible functionality.

5.3. siRNA transfection and shRNA lentiviral infection in NTera2 cells

The first strategy to knock-down PTDSR was done by siRNA transfection. As shown in Fig.11, siRNA transfection in NTera cells displayed no satisfactory knock-down of PTDSR as its levels remained nearly unchanged when examined by RT-qPCR. Therefore, a more powerful strategy was applied to achieve a higher degree of knock-down, which is the pLL3.7 shRNA lentiviral system. By efficiently depleting PTDSR, a clear picture of PTDSR target genes was obtained.

5.4. mRNA profiling revealed PTDSR regulation of critical Hox and neural genes

The microarray (Fig.14) showed a varied inducibility of the genes up- or down-regulated under RA treatment. Further analysis of the up-regulated pool of genes indicated the robust activation by RA of many of the Hox and neural genes which also required PTDSR. A systematic analysis of the PTDSR effects on the expression of all 39 Hox genes in NTera2 cells was performed. RA is a potent activator of Hox and neural gene expression (Voss AK et al, 2009). The genes in Hox clusters are activated in a temporal and spatial pattern following their genomic topography; genes at the 3'end of the clusters are activated first early on in the most anterior parts of the developing embryo, whereas genes located at progessively more 5'positions are activated subsequently during development in the more posterior areas (Kmita M et al, 2003; Deschamps J et al, 2005). Interestingly, the earlier Hox genes located at the 3'end were mostly positively regulated by PTDSR , the later ones showed a rather mixed pattern, being not inducible by RA in the time of 72 hours and either repressed, activated, or unaffected through PTDSR.

As mentioned above, PTDSR knock-down in mice resulted in severe malformations of the neural organs; Dlx5, Pax6, COUP-TF I and II, as well as CoREST2 and CNTN2 among other neural genes, play an important role in establishing neural identity (Chung IH et al, 2010; Li T et al, 2006; Belyaey ND et al, 2004; Fernandez-Rachubinski F et al, 2001; Gajovic S et al, 1997). Interestingly, the neural target genes identified in the microarray could all be validated by RT-qPCR and all required PTDSR for their activation by RA.

To determine a more complete picture of PTDSR function, an alternative transcriptome assay could be employed to generate a comprehensive gene expression dataset. High-throughput sequencing (Illumina, SOLiD, 454) has recently been employed to simultaneously measure transcript levels in cells in an unbiased fashion (Levin JZ, et al 2010). The advantages of this approach are readily observable, as sequencing is independent of microarray probe selection bias, and can assay multiple types of co-transcriptional regulation at once, from gene expression levels to splicing and non-coding RNA levels. More specifically, high-throughput RNA-seq would be employed in NTera2 cells under basal and RA-stimulated conditions, as well as infected by control or PTDSR shRNA.

5.5. Possible mechanisms of PTDSR regulation

5.5.1. H1K26me3 occupancy on selected Hox genes

To understand the underlying mechanism how PTDSR regulates the expression of the Hox and neural genes tested above, its potential enzymatic activities were considered. PTDSR belongs to the JmjC-domain containing protein superfamily, which have been shown to possess demethylase activities towards histone or non-histone methylation substrates (Tsukada Y et al, 2006). Specifically, PTDSR was shown to demethylate Histone H3 arginine 2 and Histone H4 arginine 3 residues both in vitro and in vivo (Fadok VA et al, 2000; Chang B et al, 2007). However, this activity was controversially discussed afterwards as shown by several other studies (Hahn P et al, 2010). Hahn P et al. proposed that PTDSR was unlikely to be involved in demethylating mono-, di-, and trimethylation states of H3K4, H3K9, H3K27, H3K36, and H4K20 histone residues in wildtype and Jmjd6-knockout cells. More recent studies identified PTDSR to interact with splicing regulatory proteins and to modify some of these by posttranslational hydroxylation (Hahn P, 2010; Weber CJ, 2009). Interestingly, studies in the Rosenfeld laboratory demonstrated in in vitro demethylase assays that this enzyme nevertheless had potential demethylase activity towards lysine 26 methylation on histone H1, the linker histone, (personal communication). This methylation marker has been shown to be associated with transcription repression through binding with HP1 and L3MBTL1 (West LE et al, 2010; Trojer P et al, 2009).

In this thesis it was demonstrated that PTDSR is able to bind to promoters containing H1K26me3 and possibly demethylates this mark on HoxA2, B2, B5, C5 and D3 (Figure 23 and 24). Similarly, PTDSR was found to bind to the promoter regions of selected neural genes METRN, COUPTF II, CoREST, Pax6 and Dlx5, which also showed a significantly increased occupancy of H1K26me3 under PTDSR knock-down conditions (Fig.24 and 25).

5.5.2. PTDSR regulation through direct binding

The changes in Hox gene expression upon shPTDSR infection suggested that PTDSR either regulated Hox gene expression directly or acted as a transcriptional co-regulator for Hox proteins. ChIP experiments were conducted to test the direct regulation hypothesis, and it was shown that PTDSR binding across Hox promoters was not uniform. It rather showed a different way of binding in the experiments with and without RA stimulation, respectively. The Hox genes HoxA5, A6, B5, D3 and D11 show a strong binding of PTDSR without RA treatment (Fig.23). PTDSR binding was even weaker with RA stimulation, suggesting that in those cases RA induced a pathway that prevented the direct effects of PTDSR.

An interesting future experiment would be assaying a time-course of PTDSR binding to promoters of Hox genes during RA treatment of Ntera2 cells. If these particular Hox genes that seem to dismiss PTDSR at 72h of RA treatment continue the same trend, it would represent a time-dependent progression of PTDSR deregulation. Alternatively, PTDSR could be recruited at a later timepoint, or even have a cyclic binding profile, which would engender further investigation.

5.5.3. PTDSR functions as a possible demethylase

Recent reports on the JmjC domain as a novel demethylase signature motif (Tsukada Y et al, 2006) and the discovery that many proteins containing JmjC domains are capable of reversing histone methylation marks (Klose RJ et al, 2006; Klose RJ et al, 2007) have raised the question whether PTDSR (JMJD6) also has demethylase features. However, most of the mechanisms of how these proteins function on a molecular basis have remained difficult to unravel and to predict their enzymatic targets based on sequence comparisons and analysis of their JmjC domains.

Demethylases are so far known to regulate genes that have been repressed or activated through methylation. H1 lysine 26 methylation is mainly linked to transcriptional repression which can be reversed by demethylating that specific site. Data from the Rosenfeld laboratory showed that PTDSR could remove the H1 lysine 26 repressive methylation marker in *in vitro* demethylase assays. This is a very striking finding, since it was reported that PTDSR (JMJD6) was an arginine demethylase

(Chang B et al, 2007). As shown in Fig.23, depletion of PTDSR led to increased levels of H1K26me3 on the promoter regions of selected Hox and neural genes, suggesting an *in vivo* role of PTDSR by demethylating this repressive marker. Methylation increased under siPTDSR on the promoter regions of some Hox genes as well as the examined neural genes METRN, Coup-TFII, CoREST,Pax6 and DlX5. Not all of the Hox examples can be simply explained by the RA-dependent recruitment of PTDSR, as in some cases PTDSR occupancy levels were either unchanged or even decreased upon RA treatment, suggesting a more complex mechanism. In the cases where no specific PTDSR-binding was observed, it indicates indirect regulation of those genes through other mechanisms. Future ChIP experiments will aim to see whether H1K26me3 is removed on these genes when the cells were stimulated with RA, at which condition, PTDSR is also recruited. If it is shown that H1K26me3 levels are unchanged by RA treatment, several different mechanisms could explain the changes in gene expression. PTDSR may be demethylating a different histone mark, or a non-histone protein entirely.

5.5.4. Hox gene regulation and the role of non-coding RNAs

Chromatin immunoprecipitation (ChIP) assays revealed that several Hox genes are direct targets of the demethylases UTX and JMJD3 in a variety of cell lines (Hahn P et al, 2008; Tsukada et al, 2006; Daujat S et al, 2005). UTX and JMJD3 demethylate gene-inactivating H3K27 dimethyl and trimethyl marks and are involved in inducing and/or maintaining gene expression (Hübner MR et al, 2011). Furthermore, Lan F and colleagues performed ChIP on ChIP analysis (ChIP followed by hybridization to ultra-dense tiling microarrays) on all four human Hox clusters. Combined ChIP data indicate that UTX (and probably JMJD3) selectively occupies transcription start sites of the target genes in a cell type-specific manner, so that UTX and JMJD3 positively correlate with the transcriptional activity of the promoters. These results show that Hox genes are direct targets of demethylases in the jumonji family, and I propose that PTDSR also exhibits a similar function.

Hox regulation by noncoding RNAs is an extremely active field of research, recent findings of Gupta RA et al (2010) and Rinn JL et al (2007) have found noncoding RNAs (ncRNA) to participate in the epigenetic regulation of Hox genes. These ncRNAs are

unique sequence motifs and, although still poorly understood, their expression has been shown to demarcate broad chromosomal domains of differential histone methylation and RNA polymerase accessibility. Rinn JL et al. have characterized the transcriptional landscape of the four human HOX loci and identified 231 HOX ncRNAs that extend known transcribed regions by more than 30 kilobases. They identified a 2.2kb ncRNA residing in the HOXC locus, termed HOTAIR (Hox Antisense Intergenic RNA) (Fig.26).

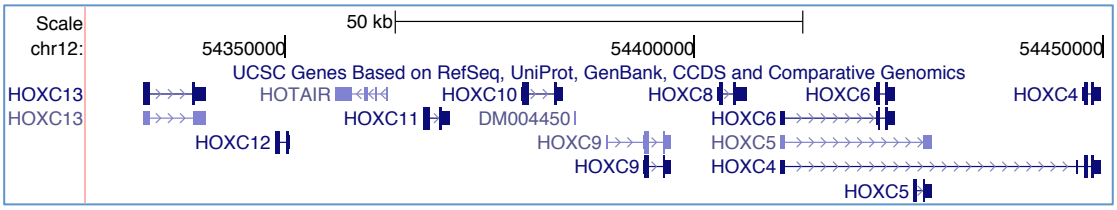

Fig.26: UCSC genome browser view of HoxC : RefSeq of HoxC cluster on chromosome 12, showing HOTAIR position (http://genome.ucsc.edu).

The ncRNA HOTAIR was detected to repress transcription in *trans* across 40 kilobases of the HoxD locus. HOTAIR is required for PRC2 (Polycomb Repressive Complex 2) occupancy and histone H3 lysine-27 trimethylation (H3K27) of HoxD. Remarkably, this transcript acts not in *cis* on the HoxC genes, but in *trans* on the HoxD complex. siRNA knock-down of HOTAIR expressed from the HoxC locus had no effect of HoxC, but lead to derepression in *trans* of a large domain of the HoxD locus. This derepression was accompanied by loss of PcG protein binding and loss of repressive histone H3 lysine 27 methylation. In the results of this thesis the inducibility of Hox genes through RA was investigated and showed a very mixed pattern as mentioned above. The tendency goes towards the “late” genes being less or not at all inducible by RA, whereas the “early” Hox genes seem to be activated rather continuously. Taken together, the existence of ncRNAs in many chromosomal domains of histone methylation as well as the close vicinity of HOTAIR to HoxC cluster could possibly be a reason for why PTDSR presents this mixed regulatory pattern. The potential for noncoding transcripts being mediators of trans-activation at Hox genes and other loci certainly is worth further investigation.

To determine the regulatory capability of PTDSR on HOTAIR, similar RT-qPCR and ChIP experiments can be performed on the HOTAIR transcript and promoter, respectively. Specifically, HOTAIR expression would be assayed in Ntera2 cells in -/+RA conditions, with and without shPTDSR. H1K26me3 levels would also be assayed under the same conditions. Depending on the type of effect that PTDSR has

on HOTAIR levels, an additional indirect layer of regulation can be described on the HoxD locus.

Interestingly, PTDSR has recently been shown to be able to bind single-stranded RNA (Hong X et al, 2010). If true, then the possible binding of PTDSR to HOTAIR should be tested using an RNA-immunoprecipitation (RIP) assay, which measures the affinity of a specific protein for any expressed RNA in cells. This experiment would have to be done in 293T cells to take advantage of the Flag-PTDSR construct described earlier, and HOTAIR expression would have to be checked in these cells. However, if HOTAIR is not expressed, then a construct containing the ncRNA gene can be transfected into these cells, allowing the RIP assay to be done.

5.6. Critical analysis of the data

Several aspects of the data presented here can be improved upon, through either utilizing more current technologies not available at the time of execution or a more thorough investigation of the preliminary findings. Some Hox gene experiments should be optimized to obtain significant data, as the current set of conditions or primers did not give consistent data. Additionally, described below are various approaches for a more complete understanding of PTDSR function.

5.6.1. Further validation of PTDSR-dependent regulation

Although the RT-qPCR experiments generally showed a clear trend of positive regulation of gene expression by PTDSR, presumably by a putative H1K26me3 demethylase activity, several assays should be conducted to reinforce the current conclusions. A rescue experiment should be designed wherein a stable Ntera2 cell line has PTDSR knocked out, and subsequently transfected with a construct expressing normal PTDSR to determine if the knock-down experiments are validated. The purpose is to eliminate the possibility that PTDSR shRNA somehow specifically caused these regulatory effects without needing PTDSR knock-down. Alternatively, if it is too difficult to construct these stable cells, multiple other PTDSR shRNAs targeting different sequences can be tested, thus reducing the chance that a specific shRNA sequence was giving a false positive result.

However, making these stable cell lines with PTDSR knock-out would be advantageous to test other aspects of PTDSR regulatory mechanisms. For example, if the rescue experiments work as expected, then various mutations could be introduced to abrogate the enzymatic portion of PTDSR to test if, indeed, the demethylase activity is required for PTDSR regulation of Hox genes and neural genes. Additionally, various isoforms of PTDSR could be tested to see if these have differential effects on Hox and neural gene regulation. At least 3 isoforms are annotated currently (Fig.27), the various functions of which are unknown.

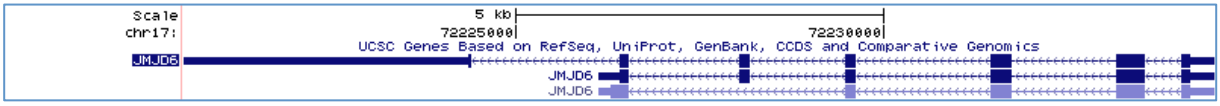

Fig.27: UCSC genome browser view of PTDSR and its 3 isoforms (http://genome.ucsc.edu).

The middle isoform, which was used for the Flag-PTDSR construct to conduct ChIP experiments in this thesis, seems to be mostly expressed in hematopoietic progenitors cells, as well as various cancer types. The bottom isoform has a similar expression pattern, but is missing exon 5. The top isoform contains the same coding region as the middle one, but has a very large 3' untranslated region (UTR) that is different from the middle isoform, which might explain its differential expression pattern, which is predominantly fetal brain tissues. Such a large discrepancy between 3'UTRs could result in differential microRNA regulation, and presents an open question for regulation of PTDSR expression itself.

5.6.2. High-throughput sequencing

Although the gene expression microarrays used in this thesis represent a large amount of data, current sequencing technologies far outpace the value of these particular microarray experiments. A single high-throughput sequencing run can produce millions of reads from which many different types of quantitative data can be obtained. For the purposes of PTDSR regulation, RNA-seq would be the most efficient sequencing type, and given enough sequencing depth, gene expression, ncRNA expression, and splicing variants can be quantified. Specifically, RNA-seq would be conducted in Ntera2 cells in -/+RA conditions, with or without shPTDSR. The data obtained from these experiments would provide a complete list of all genes regulated by RA, and any that are PTDSR-

dependent. Additionally, ncRNAs (such as HOTAIR) can all be simultaneously detected, and splicing isoforms can be analyzed (Levin JZ et al, 2010). The splicing isoforms are especially interesting because of the association between PTDSR and the splicing factor U2AF65 (Weber CJ et al, 2009), and the published enzymatic activity of this enzyme on this splicing factor.

5.6.3. Viral system to introduce Flag-PTDSR in Ntera2 for examining its binding on the promoter region of selected target genes

To facilitate examining the binding of PTDSR, a viral system will be applied to introduce it into NTera2 cells. Specifically, a control protein GFP or PTDSR will be cloned into pBobi viral vector and then co-transfected with the packaging vectors, CMV-VSVG, RSV-Rev and pMDLg/pRRE, into HEK293T cells to produce viruses for NTera2 cell infection. Infected cells will then be treated with RA for various time points followed by ChIP assay with Flag antibody to check its binding on those target genes identified through mRNA profiling experiments.

6. Summary

Epigenetic regulation has become a domain of growing interest especially in cancer research and other fields for the past years due to evolving knowledge and better research techniques in this field. Covalent modifications on histones play a fundamental role in the regulation of chromatin dynamics and function as being part of transcriptional activation or repression. One of the many post-translational modifications taking place in the genome is histone methylation, which has been shown to play a critical role in gene transcription.

Not until recently, the enzymes capable of removing these methylation marks, either on histones or non-histones, were identified. LSD1 was the founding member of demethylases, which directly reverses histone H3K4 or H3K9 modifications by an oxidative demethylation reaction in which flavin is a cofactor. In addition, the largest classes of demethylases enzymes, which contain a Jumonji C (JmjC) domain have been identified. While LSD1 can only remove mono- and dimethyl lysine modifications, the JmjC-domain-containing histone demethylases (JHDMs) are capable of reversing all three histone lysine methylation states.

Experiments carried out on JMJD6 (PTDSR) “knock-out” mice indicated that PTDSR plays an important role in tissue differentiation during embryogenesis. Delays and defects in terminal differentiation of the kidney, intestine, liver and lung during embryogenesis, brain malformation (midbrain, brainstem cord junction, and cerebellum) or bilateral absence of eyes among others were detected in the homozygote JMJD6-/- mice (Fig.04).

The major aim of this project was to identify possible biological targets for the JmjC-domain containing enzyme PTDSR. The focus was set on the possibility of Hox genes being biological targets for PTDSR, because they encode for proteins regulating important transcription factors, greatly affecting epigenetic regulation and development during embryogenesis. Also, selected neural genes were examined in this study as potential PTDSR targets.

Indeed, the experiments indicated that under RA stimulation, many of the Hox genes required PTDSR for their full activation. In contrast, some showed impaired activation or even repression when knocking down PTDSR (Fig.16). Interestingly, all the neural

genes we examined required PTDSR for their full neuronal differentiation by RA. Furthermore, PTDSR seemed to regulate many of these genes through directly binding to the promoter regions as revealed by ChIP assays, possibly through demethylating a potentially repressive histone marker, H1K26me3.

Further investigations in this field will give a more detailed insight into whether this enzyme possibly also demethylates other non-histone substrates or if it might work through complex activation in regulating gene transcription.

ZUSAMMENFASSUNG

Unter epigenetischer Regulation versteht man unterschiedliche molekulare Mechanismen, die ohne Veränderung der DNA-Nukleotidsequenz die Expression verschiedener Gene regulieren können und vererblich sind. Durch ein tieferes Verständnis und verfeinerte Forschungstechniken wird das Feld der epigenetischen Regulation für die Entwicklungsbiologie und die Krebsforschung immer wichtiger. Die Gentranskription wird neben anderen Mechanismen besonders auch durch Modifikationen an Histonen, z.B. eine Histonmethylierung, gesteuert. Eine der zuerst studierten Demethylasen, die Methylierungsmarker von Histonen entfernen können, LSD1, demethyliert oxidativ die Histone H3K4 und H3K9 am Lysin. Zusätzlich wurde eine große Klasse von Demethylasen charakterisiert, die eine Jumonji C Domäne (JmjC) enthalten und ebenfalls Lysinreste demethylieren kann. Während LSD1 nur Mono- oder Dimethyl-Lysine demethylieren kann, sind die JmjCs in der Lage alle drei Methylierungsstellen der Lysine revertieren.

Experimente mit knock-out Mäusen hatten gezeigt, dass lebenswichtige Gewebedifferenzierungsschritte in unterschiedlichen Organen (Niere, Darm, Leber, Lunge, Gehirn und Auge) durch die JmjC enthaltenden Demethylase JMJD6 (PTDSR) gesteuert werden.

In der vorliegenden Arbeit wurden potentielle Target-Gene der Demethylase JMJD6/PTDSR identifiziert. Der spezifische Fokus wurde nach der Microarray Analyse auf die Gruppe der HOX Gene gelegt, welche sich durch PTDSR deutlich regulierbar zeigten. Als Hauptziel dieser Arbeit wurde daher untersucht, ob HOX-Gene und einige neurale Gene Zielstrukturen von PTDSR enthalten, da diese wichtige Transkriptionsfaktor-regulierende Gene repräsentieren und so die epigenetische Genregulation während der Embryogenese steuern.

Die Experimente dieser Arbeit konnten zeigen, dass viele HOX-Gene, unter Stimulation mit Retiniolsäure (RA), PTSDR zur vollen Aktivität benötigen und unter knock-down Bedingungen für PTSDR funktionell inaktiv sind. Ebenso benötigen alle untersuchten neuralen Gene PTSDR zu ihrer Aktivierung durch RA. ChIP Assays zeigten, dass PTSDR bei seiner regulativen Aktivität direkt an Promotorregionen dieser Gene gebunden ist und einen potentiell repressiven Histonemarker, H1K26me3 demethyliert.

Diese Experimente sind für das molekulare Verständnis der Organentwicklung in der Embryogenese von wesentlicher Bedeutung. Weitere Experimente werden zeigen ob PTSDR auch andere Non-Histon Substrate demethyliert oder ob komplexere Regulationsmechanismen der Gentranskription greifen.

7. Outlook

Because of the prominent influence demethylases have on the transcriptional activity of genes, current studies in this field are advancing very rapidly. Many research groups are trying to identify the unique function of the individual candidates in this whole mechanism. During this work a few new perspectives and ideas for future research developed that could not be pursued due to time constraints. The preliminary ChIP experiments indicate the possible function of PTDSR and next steps in investigation are briefly outlined below as future experiments:

a) Since the binding of PTDSR was checked in HEK293T cells due to the difficulty of transfecting NTera2 cells, future study will be using a lentiviral system to introduce PTDSR into NTera2 cells followed by ChIP to further validate the binding of PTDSR on the Hox and neural genes focused in this study.
b) The exact mechanism whether PTDSR acts alone or in a complex is a key question to address. In order to understand how/why PTDSR functions as a co-repressor, it will be necessary to identify its associating partners through complex purification. A cell line stably expressing Flag-PTDSR will be generated followed by affinity purification and mass spectrometry to identify binding partners. This approach could also be useful for identifying protein targets of enzymatic functions of PTDSR.
c) In order to further investigate the enzymatic function of PTDSR in vivo, it would be necessary to check the H1K26me3 occupancy by ChIP under RA stimulation on the Hox and neural genes. This experimental set-up allows insight into the specific demethylase activity of PTDSR during gene activation.
d) To provide a more complete picture of PTDSR-dependent regulation, high-throughput sequencing of RNA species in Ntera2 cells will be conducted. In addition to gene expression targets, ncRNA and splicing targets can also be identified.

The characterized features of PTDSR will make it possible to draw a more detailed picture of the regulatory processes involved in gene expression. Because of the predominantly activating, as well as the inactivating, function of PTDSR, it is an interesting target to control gene transcription in the future. The knowledge growing from understanding the molecular regulation of these groups of enzymes and whether they can be selectively manipulated, may be of therapeutic value in human diseases.

8. References

Agger K, Cloos PA, Christensen J et al UTX and JMJD3 are Histone demethylases involved in Hox gene regulation and development. Nature 2007;449:732-734.

Anand R, Marmostein R. Structure and mechanism of lysine specific demethylase enzymes. J. Biol. Chem. 2007;282:35425-35429.

Ballas N, Battaglioli E, Atouf F et al. Regulation of neuronal traits by a novel transcriptional complex. Neuron 2001;31:353-365.

Bannister AJ, Schneider R, Kouzarides T. Histone methylation: dynamic or static. Cell 2002;109:801−806.

Barde I, Salmon P, Trono D. Production and Titration of Lentiviral Vectors. Current Protocols in Neuroscience 2010;23:4.21.1-4.21.

Bedford MT, Richard S. Arginine methylation an emerging regulator of protein function. Mol Cell. 2005;18(3):263-72.

Belyaey ND, Wood IC, Bruce AW et al. Distinct RE-1 silencing transcription factor-containing complexes interact with different target genes. J Biol. Chem. 2004;278:556-561.

Böse J, Gruber AD, Helming L, et al. The phosphatidylserine receptor has essential functions during embryogenesis but not in apoptotic cell removal. J Biol. 2004;3:15 doi: 10.1186/jbiol10

Briscoe J, Pierani A, Jessell TM, Ericson J. A homeodomain protein code specifies progenitor cell identity and neuronal fate in the ventral neural tube. Cell 2000;101:435-455.

Cao R, Wang L, Wang H et al. Role of histone H3 lysine 27 methylation in polycomb-group silencing. Science 2002;298:1039−1043.

Carroll SB. Homeotic genes and the evolution of arthropods and chordates. Nature 1995;376:479–85.

Chang B, Chen Y, Zhao Y et al. JMJD6 is a histone arginine demethylase. Science 2007;318:444-447.

Christensen J, Agger K, Cloos PA et al. RBP2 belongs to a family of demethylases, specific for tri-and dimethylated lysine 4 on histone 3. Cell 2007;128,1063-76.

Chung IH, Han J, Iwata J et al. Msx1 and Dlx5 function synergistically to regulate frontal bone development. Genesis 2010;48:645-655.

Cikala M, Alexandrova O, David CN et al. The phosphatidylserine receptor from Hydra is a nuclear protein with potential Fe(II) dependent oxygenase activity. BMC Cell Biol 2004;5:26-36.

Clifton IJ, McDonough MA, Ehrismann D et al. Structural studies on 2-oxoglutarate oxygenases and related double-stranded beta-helix fold proteins. J Inorg Biochem 2006;100:644-669.

Cloos PA, Christensen J, Agger K et al. The putative oncogene GASC1 demethylates tri- and dimethylated lysine 9 on histone H3. Nature 2006;442:307-11.

Coyle DE, Li J, Baccei M. Regional Differentiation of Retinoic Acid-Induced Human Pluripotent Embryonic Carcinoma Stem Cell Neurons. PLoS ONE 2011;6:e16174. doi:10.1371

Cui P, Qin B, Liu N et al. Nuclear localization of the phosphatidylserine receptor protein via multiple nuclear localization signals. Exp Cell Res 2004, 293:154-163.

Daujat S, Zeissler U, Wadmann T et al. HP1 binds specifically to Lys26-methylated histone H1.4, whereas simultaneous Ser27 phosphorylation blocks HP1 binding. J Biol Chem. 2005;280:38090-38095.

De Santa F, Totaro MG, Prosperini E et al. The histone H3 lysine-27 demethylase Jmjd3 links inflammation to inhibition of polycomb-mediated gene silencing. Cell 2007;130:1083-1094.

Delcuve GP, Rastegar M, Davie JR. Epigenetic control. J Cell Physiol. 2009;219(2):243-50.

Deschamps J, van Nes J. Developmental regulation of the Hox genes during axial morphogenesis in the mouse. 2005;132,2931-2942.

Drossopoulou G, Lewis KE, Sanz-Ezquerro JJ et al. A model for anteriorposterior patterning of the vertebrate limb based on sequential long- and short-range Shh signaling and Bmp signaling. Development 2000;127:1337-1348.

Duester G. Retinoic acid synthesis and signaling during early organogenesis. Cell 2008;134(6):921-931.

Emre NC, Berger SL. Histone post-translational modifications regulate transcription and silent chromatin in Saccharomyces cerevisiae. Ernst Schering Res Found Workshop 2006;57:127-53.

Fadok VA, Bratton DL, Rose DM et al. A receptor for phosphatidylserine- specific clearance of apoptotic cells. Nature 2000;405:85-90.

Fernandez-Rachubinski F, Fliegel L. COUP-TFI and COUP-TFII regulate expression of the NHE through a nuclear hormone responsive element with enhancer activity. Eur J Biochem 2001;268:620-634.

Fischle W, Wang Y, Allis CD. Histone and chromatin crosstalk. Curr Opin Cell Biol. 2003;15:172−183.

Fodor BD, Kubicek S, Yonezawa M et al. Jmjd2b antagonizes H3K9 trimethylation at pericentric heterochromatin in mammalian cells. Genes Dev 2006; 20:1557-62.

Gajovic S, St-Onge L, yokota Y et al. Retinoic acid mediates Pax6 expression during in vitro differentiation of embryonic stem cells. Differentiation 1997;62:187-192.

Gary JD, Clarke S. RNA and protein interactions modulated by protein arginine methylation. Prog nucleic acid Res Mol Biol. 1998;61:65-131.

Gedford MT, Richard S. Arginine methylation an emerging regulator of protein function. Mol Cell 2005;18:263-72.

Gupta RA, Sha N, Wang KC et al. Long non-coding RNA HOTAIR reprograms chromatin state to promote cancer metastasis. Nature 2010;464:1070-1076.

Hahn P, Boese J, Edler S et al. Genomic structure and expression of Jmjd6 and evolutionary analysis in the context of related JmjC domain containing protein. BMC Genomics 2008;9:293.

Hahn P, Wegener I, Burrells A et al. Analysis of Jmjd6 Cellular Localization and Testing for its Involvement in Histone Demethylation. PLoS One 2010;5:e13769.doi10.1371.

Hohenester E. Structural insight into Slit-Robo signalling. Biochem Soc Trans. 2008;36:251-256.

Hombria JC, Lovegrove B Beyond homeosis-HOX function in morphogenesis and organogenesis. International Society of Differentiation 2003;71:461-476.

Hong JR, Lin GH, Lin CJ et al. Phosphatidylserine receptor is required for the engulfment of dead apoptotic cells and for normal embryonic deveopement in zebrafish. Development. 2004;131(21):5417-5427.

Hong X, Zangb J, Whitec J et al. Interaction of JMJD6 with single-stranded RNA. Proc Natl Acad Sci USA 2010; 107: 14568–14572.

Hsia DA, Tepper DA, Pochampalli MR et al. KDM8, a H3K36me2 histone demethylase that acts in the cyclin A1 coding region to regulate cancer cell proliferation. Proc Natl Acad Sci USA 2010;107,9671-6.

Huang DW, Sherman BT, Lempicki RA Systematic and integrative analysis of large gene lists using DAVID bioinformatics resources. Nature Protocols 2009;4,44–57.

Hübner MR, Spector DL. Role of H3K27 Demethylases Jmjd3 and UTX in Transcriptional Regulation. Cold Spring Harb Quant Biol 2011 (Epub ahead of print)

Iwase S, Lan F, Bayliss P et al. The X-linked mental retardation gene SMCX/JARID1C defines a family of histone H3 lysine 4 demethylases. Cell 2007;128:1077-88.

Jenuwein T, Allis CD. Translating the histone code. Science 2001;293:1074−1080.

Jepsen K, Solum D, Zhou T et al. SMRT-mediated repression of an H3K27 demethylase in progression from neural stem cell to neuron. Nature 2007;450,415-9.

Katho M. Identification and characterization of JMJD2 family genes in silico. Int. J. Oncol. 2004;24:1623-1628.

Keith D. R. DNA methylation and human disease. Nature reviews 2005;6:597-611.
Klose RJ, Kallin EM, Zhang Y. JmjC-domain-containing proteins and histone demethylation. Nat Rev Genet 2006;7:715-727.

Klose RJ, Zhang Y. Regulation of histone methylation by demethylimination and demethylation. Nat Rev Mol Cell Biol 2007;8:307-318.

Kmita M, Duboule D. Organizing axes in time and space; 25 years of collinear tinkering. Science 2003;301:331-333.

Kouzarides T. Histone methylation in transcriptional control. Curr Opin Genet Dev 2002; 12:198−209.

Krieser RJ, Moore FE, Dresnek D et al. The Drosophila homolog of the putative phosphatidylserine receptor functions to inhibit apoptosis. Development 2007;134:2407-2414.

Krogan NJ, Kim M, Tong A et al. Methylation of histone H3 by Set2 in Saccharomyces cerevisiae is linked to transcriptional elongation by RNA polymerase II. Mol Cell Biol 2003;23:4207−4218.

Kunisaki Y, Masuko S, Noda M et al. Defective fetal liver erythropoiesis and T lymphopoiesis in mice lacking the phosphatidylserine receptor. Blood 2004;103:3362-4.

Lachner M, Jenuwein T. The many faces of histone lysine methylation. Curr Opin Cell Biol. 2002;14:286−298.

Lachner M, Sengupta R, Schotta G, Jenuwein T. Trilogies of histone lysine methylation as epigenetic landmarks of the eukaryotic genome. Cold Spring Harb Symp Quant Biol 2004;69:209−218.

Lan F, Bayliss PE, Rinn JL et al. A histone H3 lysine 27 demethylase regulates animal posterior development. Nature 2007;449,689-94.

Lan F, Nottke A, Shi Y. Mechanisms involved in the regulation of histone lysine demethylases. Current Opinion in Cell Biology 2008;20:316–325.

Lee DY, Teyssier C, Strahl BD, Stallcup MR. Role of protein methylation in regulation of transcription. Endocr. Rev. 2005;26:147-170.

Lee MG, Villa R, Trojer P et al. Demethylation of H3K27 regulates polycomb recruitment and H2A ubiquitination. 2007 Science;318:447-450.

Lee Y, Song AJ, Baker R et al. Jumonji, a nuclear protein that is necessary for normal heart development. Circ Res 2000;86:932-938.

Levin JZ, Yassour M, Adiconis X et al. Comprehensive comparative analysis of strand-specific RNA sequencing methods. Nature Methods 2010;9:709-15.

Li MO, Sarkisian MR, Mehal WZ et al. Phosphatidylserine receptor is required for clearance of apoptotic cells. Science 2003;302:1560-1563.

Li T, Lu Z, Lu L. Pax6 regulation in retinal cells by CCCTC binding factor. Invest Ophtalmol Vis Sci. 2006;47:5218-5226.

Margueron R, Trojer P, Reinberg D. The key to development: interpreting the histone code. Curr Opin Genet Dev 2005;5:163−176.

Liu W, Tanasa B, Tyurina OV et al. PHF8 mediates histone H4 lysine 20 demethylation events involved in cell cycle progression. Nature 2010;466:508-515.

Martin C, Zhang Y. The diverse functions of histone lysine methylation. Nat Rev Mol Cell Biol 2005;6:838−849.

Metzger E, Wissmann M, Yin N et al. LDS1 demethylates repressive histone marks to promote androgen-receptor-dependent transcription. Nature 2005;437:436-439.

Ming OL, Matthew RS, Wajahat Z et al. Phosphatidylserine receptor is required for clearance of apoptotic cells. Science 2003;302:doi:10.1126

Montavon T, Le Garrec J, Kerszberg M et al. Modeling Hox gene regulation in digits: reverse collinearity and the molecular origin of thumbness Genes and Developement 2007;22:346–359.

Murray K. The occurence of epsilon-N-methyl lysine in histones. Biochemistry 1964;3:10-15.

Nielsen SJ, Schneider R, Bauer UM et al. Rb targets histone H3 methylation and HP1 to promoters. Nature 2001;412:561−565.

Ogura T., Evans RM. A retinoic acid-triggered cascade of HOXB1 gene activation. Proc Natl Acad Sci USA 1995;92(2):387-391.

Pahlich S, Zakaryan RP, Gehring H. Protein arginine methylation: Cellular functions and method of analysis. Biochim Biophys Acta 2006; 1764:1890-1903.

Paik WK, Kim S. Enzymatic methylation of protein fractions from calf thymus nuclei. Biochem Biophys Res Commun. 196729:14-20

Peters AH, Kubicek S, Mechtler K et al. Partitioning and plasticity of repressive histone methylation states in mammalian chromatin. Mol Cell 2003;12:1577−1589.

Pleasure SJ, Lee VM. NTera 2 cells: a human cell line which displays characteristics expected of a human committed neuronal progenitor cell. Journal of Neuroscience Research 1993;35:585-602.

Reinberg D, Chuikov S, Farnham P et al. Steps toward understanding the inheritance of repressive methyl-lysine marks in histones. Cold Spring Harb Symp Quant Biol 2004;69:171−182.

Rice JC, Briggs SD, Ueberheide B et al. Histone methyltransferases direct different degrees of methylation to define distinct chromatin domains. Mol Cell 2003;12:1591−1598.

Riddle NC, Elgin SC. A role for RNAi in heterochromatin in Drosophila. Curr Top Microbiol Immunol. 2008;320:185-209.

Rinn JL, Kertesz M, Wang JK et al. Functional demarcation of active and silent chromatin domains in human HOX loci by noncoding RNAs. Cell 2007;129:1311-1323.

Robertson KD. DNA methylation and human disease. Nat Rev Genet. 2005;6(8):597-610.

Rubinson DA, Dillon CP, Kwiatkowski AV et al. A lentivirus-based system to functionally silence genes in primary mammalian cells, stem cells and transgenic mice by RNA interference. Nature genetics 2003;33:401-406.

Saeed AI, Bhagabati NK, Braisted JC et al. TM4 microarray software suite. Methods Enzymol. 2006;411:134–193.

Santos-Rosa H, Schneider R, Bannister AJ et al. Active genes are tri-methylated at K4 of histone H3. Nature 2002;419:407−411.

Sâsîk R, Woelk CH, Corbeil J. Microarray truths and consequences. J. Mol. Endocrinol. 2004;33:1–9.

Schotta G, Lachner M, Sarma K et al. A silencing pathway to induce H3-K9 and H4-K20 trimethylation at constitutive heterochromatin. Genes Dev 2004;18:1251−1262.

Schubeler D, MacAlpine DM, Scalzo D et al. The histone modification pattern of active genes revealed through genome-wide chromatin analysis of a higher eukaryote. Genes Dev 2004;18:1263−1271.

Schwender H, Ickstadt K. Empirical Bayes analysis of single nucleotide polymorphisms. BMC Bioinformatics 2008;9,144-159.

Seward DJ, Cubberley G, Kom S et al. Demethylation of trimethylated histone H3 Lys4 in vivo by JARID1 JmjC proteins. Nat Struct Mol Biol. 2007;14:240-2.

She X, Rohl CA, Castle JC et al. Definition, conservation and epigenetics of housekeeping and tissue-enriched genes. BMC Genomics 2009;10:269doi:10.1186.

Shi Y, Lan F, Matson C et al. Histone demethylation mediated by the nuclear amine oxidase homolog LSD1. Cell 2004;119:941-953.

Shi Y, Whetstine J. Dynamic Regulation of Histone Lysine Methylation by Demethylases. Cell 2007;119;941-953.

Shi Y. Histone lysine demethylases: emerging roles in development, physiology and disease. Nature Reviews Genetics 2007;8:829-833.

Shin S, Janknecht R. Diversity within the JMJD2 histone demethylase family. Biochem Biophys Res Commun. 2007;353:973-7.

Slotkin RK, Martienssen R. Transposable elements and the epigenetic regulation of the genome. Nat Rev Genet. 2007;8(4):272-285

Smith B, Treadwell J, Zhang D et al. Large-Scale Expression Analysis Reveals Distinct MicroRNA Profiles at Different Stages of Human Neurodevelopment. PLoS 2010;5:doi:10.1371.

Strahl BD, Allis CD. The language of covalent histone modifications. Nature 2000; 403:41−45.

Takeuchi T, Kojima M, Nakajima K et al. Jumonji gene is essential for the neurulation and cardiac development of mouse embryos with a C3H/He background. Mech Dev1999;86:29-38.

Tibrewal N, Liu T, Li H et al. Characterization of the biochemical and biophysical properties of the phosphatidylserine receptor (PS-R) gene product. Mol Cell Biochem 2007;304:119-125.

Toyoda M, Kojima M, Takeuchi T. Jumonji is a nuclear protein that participates in the negative regulation of cell growth. Biochem Biophys Res Commun 2000;274:332-336.

Trewick SC, McLaughlin PJ, Allshire RC. Methylation: lost in hydroxylation? EMBO Rep 2005;6:315-320.

Trojer P, Zhang J, Yonezawa M et al. Dynamic Histone H1 Isotype 4 Methylation and Demethylation by Histone Lysine Methyltransferase G9a/KMT1C and the Jumonji Domain-containing JMJD2/KDM4 Proteins. 2009;284:8395-8405.

Tsukada Y, Fang J, Erdjument-Bromage H et al. Histone demethylation by a family of JmjC domain-containing proteins. Nature 2006;439:811-816.

Tusher VG, Tibshirani R, Chu G. Significance analysis of microarrays applied to the ionizing radiation response. Proc. Natl Acad. Sci. USA 2001;98,5116–5121.

Urieli-Shoval S, Gruenbaum Y, Sedat J et al. The absence of detectable methylated bases in Drosophila melanogaster DNA. FEBS Lett. 1982;146(1):148-152.

Van Holde KE, Chromatin, Springer-Verlag, New York, 1988.

Voss AK, Collin C, Dixon MP et al. Moz and Retinoic Acid Coordinately Regulate H3K9 Acetylation, Hox Gene Expression, and Segment Identity. Developmental cell 2009;17,674-686.

Wang GG, Allis CD, Chi P. Chromatin remodeling and cancer, part I: covalent histone modifications. Trends Mol. Med. 2007;13:363-372.

Wang H, An W, Cao R et al. mAM facilitates conversion by ESET of dimethyl to trimethyl lysine 9 of histone H3 to cause transcriptional repression. Mol Cell 2003;12:475−487.

Weber CJ, Wolf A, Gromak N et al. Jmjd6 catalyses the lysyl-hydroxylation of U2AF65, a protein associated with RNA splicing. Science 2009 ;325:90-93.

West LE, Roy S, Lachmi-Weiner K et al. The MBT repeats of L3MBTL1 link SET8-mediated p53 methylation at lysine 382 to target gene repression. J Biol Chem. 2010;285:37725-37732.

Whetstine JR, Nottke A, Lan F et al. Reversal of histone lysine trimethylation by the JMJD2 family of histone demethylases. Cell 2006;125:467-481.

Yamane K, Toumazou C, Tsukada Y et al. JHDM2A, a JmjC-containing H3K9 demethylase, facilitates transcription activation by androgen receptor. Cell 2006;125:483-495.

9. Publications

Berdel AL, Henrich W. Antenatal sonographic features of Poland syndrome on 2- and 3-dimensional sonography (Letter to the editor). J Ultrasound Med 2010; 29:679-680

Die Publikation dieser Dissertation ist in Arbeit.

Mein Lebenslauf wird aus datenschutzrechtlichen Gründen in der elektronischen Version meiner Arbeit nicht veröffentlicht.

10. Acknowledgements

First of all, I want to thank Michael Geoffrey Rosenfeld and Thorsten Cramer for the tremendous opportunity to work and learn in the Rosenfeld lab at the UCSD and to write my MD thesis on such an interesting and challenging topic. I enjoyed the time in San Diego very much and appreciate the trust and patience Thorsten showed as a dream came true for me to experience a fantastic place such as San Diego – not just as a growing scientist.
Very special thanks go out to both Wen Liu and Kasey Hutt, who supported and motivated me on this project, even when times were rough. In addition, I'd like to thank all group members of the Rosenfeld laboratory, which made working on my thesis in a nice atmosphere an easier process and the whole stay worthwhile.

Ein grosser Dank gilt meinen Eltern, die mich während der ganzen Phase der Laborarbeit und besonders in der Phase des Schreibens dieser Dissertation ausserordentlich unterstützt und ermutigt haben. Auch dafür, dass ich diese Arbeit in einem herausragenden Labor in den USA anfertigen konnte und ein unglaublich lehrreiches und wunderschönes Auslandsjahr erleben durfte.

Ausserdem gilt ein ganz besonderer Dank Wilm Zunkel, der mich während der Phase des Schreibens stehts motiviert hat und mir bei den technischen Fragen und Komplikationen mit dem Computerprogamm äusserst kompetent und mit viel Passion zur Seite stand.

11. Erklärung

Hiermit erkläre ich, Ania Lisette Berdel, dass die Dissertation mit dem Titel

“Identification and characterization of potential target genes of the histone demethylase PTDSR/JMJD6”

Selbst verfasst ist und keine anderen als die angegebenen Quellen und Hilfsmittel benutzt wurden. Die Arbeit wurde ohne die unzulässige Hilfe Dritter verfasst und stellt auch in Teilen keine Kopie anderer Arbeiten dar.